



|                               |   |
|-------------------------------|---|
| <b>Publication Year</b>       | 2022  |
| <b>Acceptance in OA @INAF</b> | 2024-01-09T11:00:58Z  |
| <b>Title</b>                  | The thermal architecture of the ESA ARIEL payload at the end of phase B1                        |
| <b>Authors</b>                | MORGANTE, GIANLUCA; TARENZI, Luca; Desjonqueres, L.; Eccleston, P.; Bishop, G.; et al.          |
| <b>DOI</b>                    | 10.1007/s10686-022-09851-y  |
| <b>Handle</b>                 | <a href="http://hdl.handle.net/20.500.12386/34512">http://hdl.handle.net/20.500.12386/34512</a> |
| <b>Journal</b>                | EXPERIMENTAL ASTRONOMY  |
| <b>Number</b>                 | 53  |



# The thermal architecture of the ESA ARIEL payload at the end of phase B1

G. Morgante<sup>1</sup> · L. Terenzi<sup>1</sup> · L. Desjonqueres<sup>2</sup> · P. Eccleston<sup>2</sup> · G. Bishop<sup>2</sup> · A. Caldwell<sup>2</sup> · M. Crook<sup>3</sup> · R. Drummond<sup>2</sup> · M. Hills<sup>3</sup> · T. Hunt<sup>4</sup> · D. Rust<sup>4</sup> · L. Puig<sup>5</sup> · T. Tirolien<sup>5</sup> · M. Focardi<sup>6</sup> · P. Zuppella<sup>7</sup> · W. Holmes<sup>8</sup> · J. Amiaux<sup>9</sup> · M. Czupalla<sup>10</sup> · M. Rataj<sup>11</sup> · N. C. Jessen<sup>12</sup> · S. M. Pedersen<sup>12</sup> · E. Pascale<sup>13</sup> · E. Pace<sup>14</sup> · G. Malaguti<sup>1</sup> · G. Micela<sup>15</sup>

Received: 30 September 2020 / Accepted: 23 March 2022 / Published online: 31 March 2022  
© The Author(s) 2022, corrected publication 2022

## Abstract

The Atmospheric Remote-sensing Infrared Exoplanets Large-survey (ARIEL) is the fourth medium (M4) mission selected in the context of the ESA Cosmic Vision 2015–2025 programme, with a launch planned in 2028. During 4 years of flight operations, ARIEL will probe the chemical and physical properties of approximately 1000 known exoplanets by observing their atmosphere, to study how planetary systems form and evolve [1, 2]. The mission is designed as a transit and eclipse spectroscopy survey, operated by a 1-m class telescope feeding two instruments, the Fine Guidance system (FGS) and the ARIEL InfraRed Spectrometer (AIRS), that accommodate photometric and spectroscopic channels covering the band from 0.5 to 7.8  $\mu\text{m}$  in the visible to near-IR range [3, 4]. The mission high sensitivity requirements ask for an extremely stable thermo-mechanical platform. The payload thermal control is based on a passive and active cooling approach. Passive cooling is achieved by a V-Groove shields system that exploits the L2 orbit favourable thermal conditions to cool the telescope and the optical bench to stable temperatures  $<60$  K. The FGS focal planes operate at the optical bench temperature while the AIRS channel detectors require a colder reference, lower than 42 K. This is provided by an active cooling system based on a Neon Joule-Thomson cold end, fed by a mechanical compressor. In this paper we report the thermal architecture of the payload at the end of Phase B1 and present the requirements that drive the design together with the analyses results and the expected performances.

---

This paper is presented on behalf of the ARIEL Consortium.

---

✉ G. Morgante  
gianluca.morgante@inaf.it

Extended author information available on the last page of the article

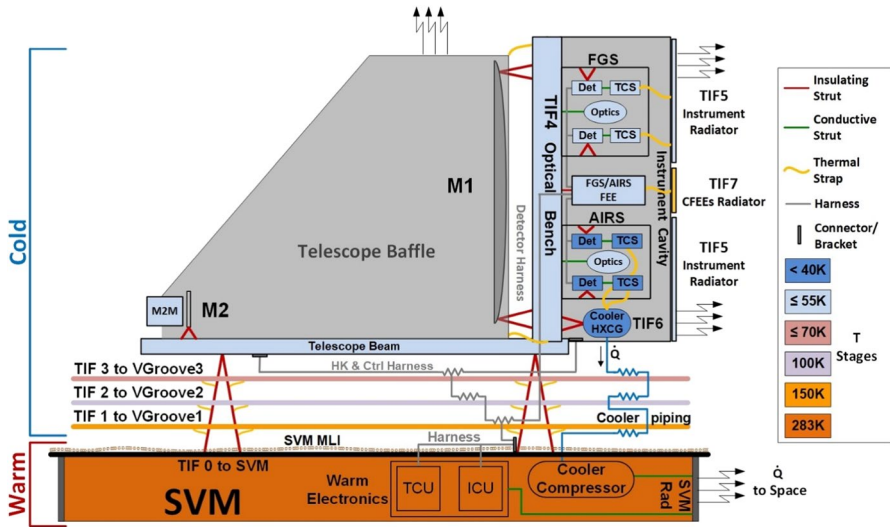


Fig. 1 PLM thermal Architecture Scheme

**Keywords** Exoplanets · Infrared spectroscopy · Thermal control · Passive cooling · Cryogenics

## 1 Introduction

### 1.1 Baseline thermal architecture and design

The spacecraft thermal design (Fig. 1) is based on a cold Payload Module (PLM) sitting on the top of a warm Service Module (SVM). The SVM is thermally controlled in the 253 K–323 K range for nominal operations of all the units of the spacecraft (S/C) and of the warm payload subsystems. The design choice to have a dedicated cold PLM was driven by the need to shield the scientific instruments and the Telescope Assembly, composed by the mirrors, the supporting struts and the optical bench, from the warm section of the S/C and to provide it with the required cooling and thermal stability at temperatures <60 K. One of the main objectives of the ARIEL cold PLM thermal design is to ensure as much as possible an isothermal environment for the Telescope Assembly. The choice of Aluminium alloy for the telescope mirrors and structures requires that all temperature differences are minimized throughout the whole telescope structure, to minimize any possible effect of different thermo-elastic deformation that could introduce unwanted optical distortions.

The ARIEL thermal control is accomplished by a combination of passive and active cooling systems. Passive cooling is achieved by a high efficiency thermal shielding system (Fig. 1 and Fig. 2) based on a multiple radiators configuration that, in the L2 environment, can provide stable temperature stages down to the 50 K range. At 1.5 million km from the Earth in the anti-Sun direction, the L2 orbit

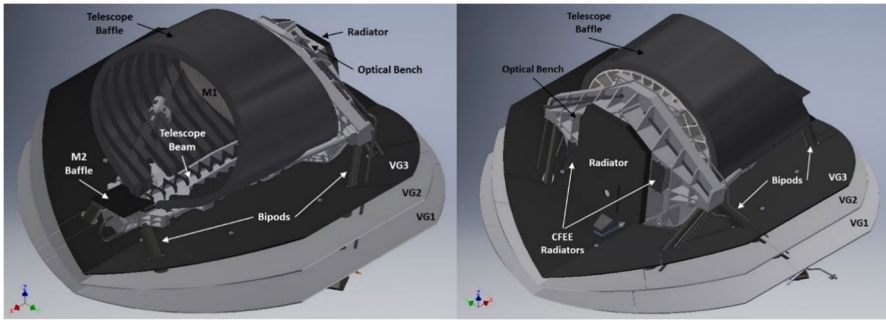


Fig. 2 ARIEL PLM thermo-mechanical architecture

allows the spacecraft to point targets distributed over the sky while maintaining the attitude within a fixed range relative to the Sun-Earth system and a limited Solar Aspect Angle (SAA) with respect to the spacecraft axes. By limiting the SAA range, ARIEL can operate in a very stable thermal environment keeping in the shade the coldest section of the PLM from the Sun/Earth/Moon illumination. For this reason, the SAA allowed during nominal observations is limited to  $\pm 5^\circ$  around the spacecraft Y-axis and to  $\pm 25^\circ$  around the X-axis. Due to possible contingencies, mainly related to the first phases of the mission, an extra margin of, respectively,  $6^\circ$  and  $5^\circ$ , has been assumed on these values: the thermo-mechanical architecture of the PLM has been designed within a total envelope of  $\pm 11^\circ$  around the spacecraft Y-axis and  $\pm 30^\circ$  around the X-axis (Fig. 3). This configuration allows to minimize the possibility of Sun illumination of the cold PLM even in during non-operational phases even before S/C attitude acquisition (e.g. LEOP) [3].

During flight operations the SVM upper platform, the main thermo-mechanical interface of the PLM to the S/C, the Payload Interface Platform (PIP), is maintained in the range 215 – 293 K and is covered with a low emissivity MLI

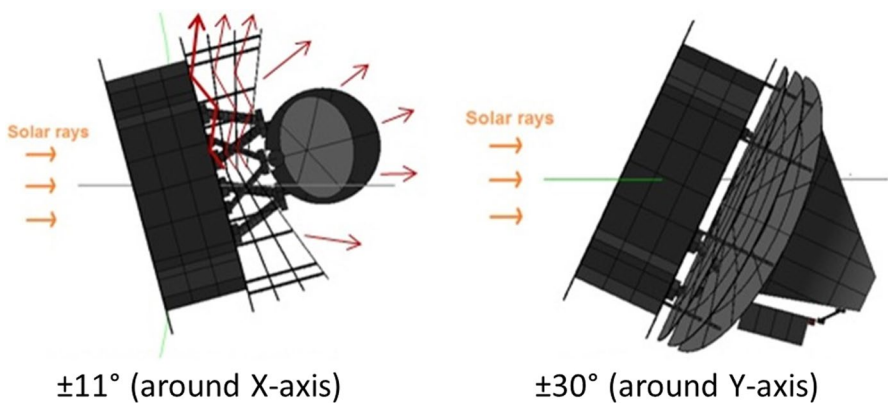


Fig. 3 ARIEL S/C attitude and SAA in orbit

blankets, acting as the first main radiative barrier between the PLM and the warm units in the service module. The geometrical configuration of the PLM passive stages and the maximum Solar Aspect Angles allowed during the mission are strongly related. The SVM interface is assumed, at this stage of the study, as a perfect Sun shield for the PLM in the thermal analysis. This assumption will be verified in the next design phase as the first Sun shielding stage and the PLM passive cooling system must be mutually designed.

As anticipated, the passive cooling system is based on a three V-Groove radiators combination (Fig. 1 and Fig. 2). They represent the first cooling stage of the PLM. Mechanically supported on the SVM by insulating struts, their shape, geometrical configuration and optical properties allow an efficient rejection of heat to cold space (Fig. 3). Past missions (Planck) have demonstrated that, in an environment such as L2, it is possible to passively reach and maintain temperatures down to the 40 K range with heat loads up to more than 1 W. On ARIEL these three radiators, called V-Groove 1, 2 and 3 (VG1, VG2, VG3), operate in sequence at temperatures around 150 K, 100 K and 60 K respectively, providing stable temperature references for the Instrument units, for the interception of the parasitic heat leaks (harness, struts, radiation) and for the active cryocooler pre-cooling. The last V-Groove, VG3, defines the coldest passive environment of the Telescope Assembly and instruments accommodated on the PLM (Fig. 2) [4, 5].

The telescope is required to operate at a temperature  $< 70$  K [6]. The Telescope Assembly (TA), enclosed in the cold environment established by the last V-Groove, acts as an extra passive stage using its large Baffle and Optical Bench (TOB) as radiating surfaces. These radiators, coated by a high IR emissivity paint, greatly improve the efficiency and the performances of the overall PLM passive cooling. The whole telescope structure and the mirrors reach, at steady state, temperatures around 50 K with only a few degrees difference between the Hot and Cold case (the two thermal analysis cases reflecting the hot and cold extremes of the nominal operations scenario), demonstrating the excellent performances of the passive cooling system in shielding the coldest PLM units from the warm sections of the S/C.

Instrument radiative thermal control is achieved by properly selecting the thermo-optical properties of the exposed surfaces. The radiative environment for the instruments is set by the Optical Bench cavity enclosed by the Instrument Radiator. In this way, the instrument optical and cold front end modules are shielded from the external environment. The Instrument Radiator, fully confined in the cold radiative environment set by the last V-Groove, during operations faces the cold space rejecting efficiently the heat loads dissipated on the optical bench. At present, the allocated area for this radiator is defined by the dimension of the open cavity that encases the instrument modules. If needed, there is margin to extend the size of the radiator area, should the passive cooling system require enhanced thermal performance. The remaining surface of the TOB, directly exposed to cold space, is black painted to maximize radiative coupling to cold sky. The internal surface of the bench cavity that accommodates the instrument modules and optics requires a black coating to minimize visible stray-light leaks. For the same reason, the module boxes are externally treated with low reflectivity coating.

The FGS and the AIRS modules ([5, 7]) share a similar thermal design (see Fig. 4). Both Instrument modules are integrated on the Optical Bench, inside the bench cavity, and include optical units incorporating the relevant detector channels. Their cooling is achieved following a diverse approach, though, according to the different temperature requirements of each frequency band. The detectors of the Fine Guidance System (FGS), located in the FGS module box are passively cooled to  $T \leq 60$  K by the Telescope Optical Bench. The ARIEL Infra-Red Spectrometer (AIRS) detectors must be operated at a colder temperature, below 42 K (see Table 1), with the goal of reaching a temperature lower than 36 K, to minimise detector noise. Maintaining this temperature, with a load of tens of mW, requires an active cooling system. The selected baseline design for the cryocooler relies on the Planck mission and EChO project study heritage: a Joule-Thomson (JT) cold end fed by a Planck-like mechanical compressor using Neon gas isenthalpic expansion to achieve the required low temperature and heat lift [5]. This Ne JT cooler is capable of producing a heat lift  $>90$  mW with margin in the expected boundary operating conditions of the ARIEL PLM. The design of the ARIEL active cooling system is under the responsibility of the Rutherford Appleton Laboratory (RAL) in the UK.

The rest of the AIRS module (box, optics etc.) will operate at the optical bench temperature, 60 K or below. For this reason, while the AIRS instrument module is thermally coupled to the OB, its Focal Plane Assembly (FPA) needs to be carefully insulated from the box, to limit the heat leak to the JT cooler cold end. In order to provide the required cooling to the AIRS detectors, the cold end heat exchanger is located in close proximity to the FPAs, to minimize the distance and the thermal strap length, and supported on the Optical Bench by insulating struts.

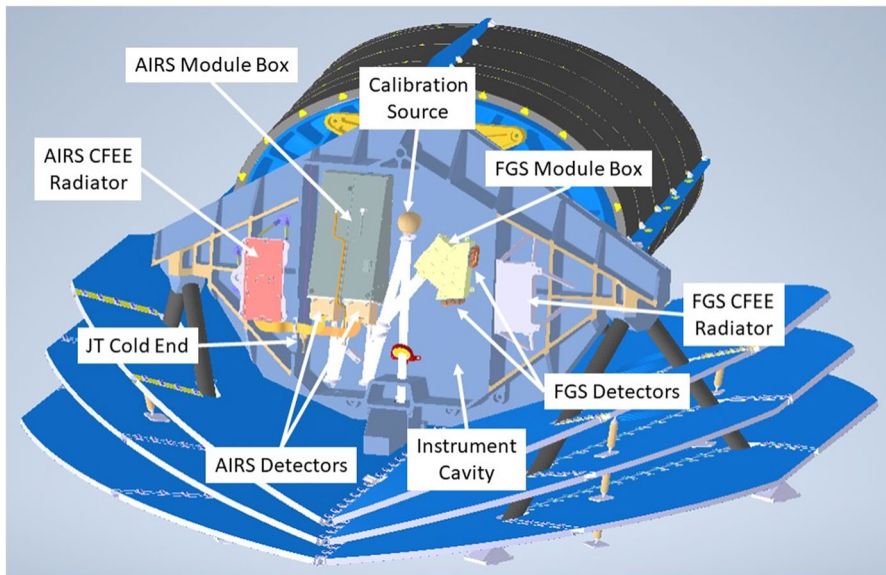


**Fig. 4** CAD view of the modules thermo-mechanical configuration on the OB

**Table 1** Main thermal requirements and expected active loads for the ARIEL payload

| ARIEL PLM Units, IFs thermal requirements and assumed active loads |                     |                      | Thermal Interface(TIF) temperatures and assumed active loads <sup>1</sup> [mW] |                     |                     |                     |                     |                     |                     |                               |
|--|---------------------|----------------------|--|---------------------|---------------------|---------------------|---------------------|---------------------|---------------------|-------------------------------|
|  |                     |                      | SVM(TIF 0)   | VG1 (TIF1)          | VG2 (TIF2)          | VG3 (TIF3)          | TOB (TIF 4)         | L_Rad (TIF5)        | JT CE (TIF 6)       | CFEE Rad <sup>8</sup> (TIF 7) |
|  | T <sub>Op</sub> [K] | $\Delta T^4$ [K]     | T <sub>Op</sub> [K]  | T <sub>Op</sub> [K] | T <sub>Op</sub> [K] | T <sub>Op</sub> [K] | T <sub>Op</sub> [K] | T <sub>Op</sub> [K] | T <sub>Op</sub> [K] |                               |
| Payload Unit   | T <sub>Op</sub> [K] | $\Delta T^4$ [K]     | 215–293 <sup>2</sup><br>145–200 <sup>3</sup>                                   | ≤ 200               | ≤ 120               | ≤ 70                | < 60                | < 60                | < 40                | > 130                         |
| Telescope  | < 70                | ± 1                  | –  | –                   | –                   | –                   | –                   | –                   | –                   | –                             |
| OB Common Optics   | ≤ 60                | ± 0.5                | –  | –                   | –                   | –                   | –                   | –                   | –                   | –                             |
| FGS Optics   | ≤ 60                | ± 0.5                | –  | –                   | –                   | –                   | –                   | –                   | –                   | –                             |
| FGS 1 detectors  | ≤ 70                | ± 0.01               | –  | –                   | –                   | –                   | 20 <sup>5</sup>     | –                   | –                   | –                             |
| FGS 2 detectors  | ≤ 70                | ± 0.01               | –  | –                   | –                   | –                   | 20 <sup>5</sup>     | –                   | –                   | –                             |
| FGS CFEE   | > 130               | ± 1 <sup>10</sup>    | –  | –                   | –                   | –                   | –                   | –                   | –                   | 400 <sup>6</sup>              |
| AIRS Optics  | ≤ 60                | ± 0.5                | –  | –                   | –                   | –                   | –                   | –                   | –                   | –                             |
| AIRS Ch0 detector  | ≤ 42                | ± 0.005              | –  | –                   | –                   | –                   | –                   | –                   | 2 <sup>5</sup>      | –                             |
| AIRS Ch1 detector  | ≤ 42                | ± 0.005              | –  | –                   | –                   | –                   | –                   | –                   | 2 <sup>5</sup>      | –                             |
| AIRS CFEE  | > 130               | ± 0.05 <sup>10</sup> | –  | –                   | –                   | –                   | –                   | –                   | –                   | 400 <sup>6</sup>              |
| JT cooler pre-cooling stage  | VG T                | NA                   | NA   | 65–180 <sup>7</sup> | 20–120 <sup>7</sup> | 40–140 <sup>7</sup> | NA                  | NA                  | NA                  | NA                            |
| Total active load <sup>1,9</sup> [mW]                              |                     |                      | 0  | 65–180              | 20–120              | 40–140              | 40                  | 0                   | 4                   | 800                           |

<sup>1</sup>Based on present estimation of expected active loads

<sup>2</sup>Conductive interface to SVM max and min T

<sup>3</sup>Radiative interface to SVM max and min T

<sup>4</sup>Peak to peak value over a typical observation time (10 h)

<sup>5</sup>FPA estimated loads, with margin, including active temperature control

<sup>6</sup>Worst Case dissipation, 200 mW per Sidecar unit

<sup>7</sup>Nominal reference values for the thermal analysis, actual load depends on VG temperatures and mass flow

<sup>8</sup>The Sidecar configuration is assumed as the baseline for both modules. CFEE Radiator is considered here as a single interface, load should be split between the two radiators

<sup>9</sup>These are the active load values assumed in the thermal analysis

<sup>10</sup>The different requirement on the temperature stability of the cold front end electronics for the two instrument modules is driven by the different sensitivity performance requirements at the level of the focal planes

In general, each detector stage is thermally decoupled from the associated instrument module, to maximize performances of the FPA in terms of absolute temperature and stability. The coupling of the detectors to the temperature reference stage (the JT cold end for the AIRS and the OB for the FGS) is achieved by means of high conductivity thermal straps made by high purity Aluminium. Active thermal control to stabilize the detectors temperature is operated by the channels Detector Control Unit (DCU), via a built-in control loop, under the responsibility of the modules development team.

The present baseline for both modules' Cold Front End Electronics (CFEE) is based on a Sidecar solution provided by NASA JPL. Due to issues during the

cryogenic qualification campaign of the Euclid SIDECAR thermo-mechanical packaging, that is the present baseline for the ARIEL channels Cold Front End Electronics (CFEE), a PLM thermal design capable of maintaining the FGS/AIRS SIDECAR at a safe temperature above 130 K is required. The AIRS team is presently working on an alternative configuration based on a discrete electronics design, that will have the advantage, from a thermal point of view, of working at the TOB temperature with no need of maintaining a safety temperature range. To date, as a sort of a possible thermal worst case condition, it has been decided to assume the Sidecar configuration for both instrument modules and all analyses and results in this paper are related to this configuration.

At this stage, the thermal analyses show that the best solution is to use a dedicated radiator for the two Sidecar of each modules. Each SIDECAR couple is directly mounted on its radiator, insulated from the OB and from the Instrument Radiator, small enough to operate, when loaded with the expected power dissipated by the electronics, at a temperature higher than 130 K. The area for both CFEE radiators is approximately 50 cm<sup>2</sup>. In order to ensure electrical performance of the detector systems, the cryo-harness connecting the electronics to the detectors cannot be longer than few tens of cm, at max. The present baseline design of the CFEEs minimizes the distance with the FPAs, with a harness length of approximately 25 cm, an acceptable value, while keeping the electronics well insulated above the cold optical bench. Figure 4 shows the TOB thermal design with the two small radiators. In all Operating Modes with the CFEE in an OFF state, the automatic activation of a survival heating line is required to ensure that the hardware is continuously maintained above the safe minimum non-operational temperature limit. This configuration is assumed as the present baseline design for the modules detectors configuration.

The warm electronics and cooler compressor are located in the SVM [8]. The cooler piping and the cryo-harness for the thermal control and for the secondary mirror mechanism (M2M), from SVM to cold PLM, should be thermally linked to all passive stages (VG1, VG2, VG3) to minimize parasitic leaks on the TOB. On the other hand, the detectors control harness (from the warm electronics to the cold proximity electronics) is thermally coupled to the VG1 only: this solution is adopted to contribute to the thermal control of the instruments CFEEs. The cables can operate as significant thermal conductors, so their heat leak into the CFEE is used as an extra passive load to maintain the electronics temperature safety limit.

## 1.2 Thermal requirements at the main interfaces

For a cryogenic instrument, internal and external thermal interfaces definition and management are the key to a successful design. The general scheme of the PLM, shown in Fig. 1, illustrates the eight main thermal interfaces of the PLM identified in the analysis: one to the S/C and the others internal to the PLM. The system thermal design has been based on the flow down of the basic instrument requirements (Table 1) to the main thermal interfaces.



The IF temperature values are fixed by the detectors/optics operating point and by the assumed total conductance from these units to their interfaces. The thermal stability requirements of the interfaces over a typical exposure time (approximately 10 h) is set to ensure the required stability of the module units. The stability across longer periods, such as seasonal or orbital changes over mission, must be taken into account when dimensioning the interfaces and the relative couplings. The requirements are defined to ensure best thermal performances of the optical and detector systems over longer periods and full mission lifetime.

The only conductive and radiative interface of the PLM to the S/C is the SVM top surface. For thermal analysis purposes, at present, this interface is assumed as a fixed boundary, fully shielding the cold PLM from Sun and warmer section of the S/C, with the following characteristics:

- Conductive coupling: temperature range 215 – 293 K (respectively, Cold and Hot Thermal Case) with a stability of 10 K over an observation period of 10 h.
- Radiative coupling: IR emissivity = 0.05, temperature range 145 – 200 K (respectively, Cold and Hot Thermal Case) with a stability of 10 K over an observation period of 10 h.

The conductance values defined in this study and assumed for the thermal analyses can be achieved using standard materials and solutions adopted already in previous experiments [9, 10]: GFRP and CFRP (with Ti alloy fixtures) for insulating struts and 5 N Al (or Cu) for the high conductivity links. Standard Al alloys (such as 6061) are used for most of PLM structures and units as well as for the telescope structure. Stainless steel (TBC) bolts (A2–70) not smaller than M4 shall be used for the main mechanical couplings to Spacecraft and to the TOB. In general, to optimize the thermal contact, the maximum bolt dimension allowed by the mechanical allocations and design should be used, in combination with spring washers. A thermal filler (Gold or Indium foil for example) could also be considered to improve conductance when needed.

## 2 Payload module thermal control hardware

The ARIEL Thermal Control Hardware (TCHW) includes all passive or active components that are used to reach and maintain the operating temperatures of the PLM units within their required ranges and stability.

The general list of the PLM TCHW items is composed by:

- *Passive Units*
  - V-Grooves (including supporting struts)
  - Bipods
  - Instrument Radiator
  - Telescope Baffle (mainly the upper half)
  - Thermal straps

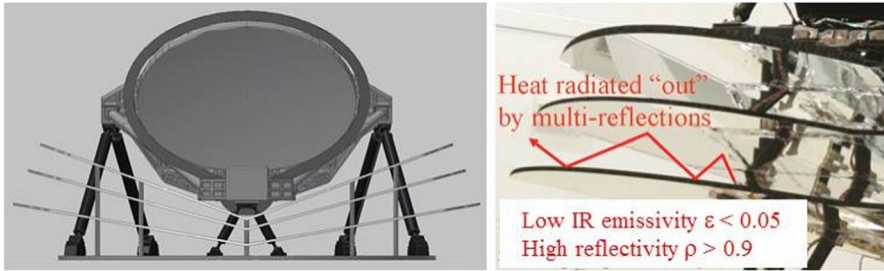


Fig. 5 ARIEL V-Grooves scheme

– *Active Units*

- Neon JT cooler
- Thermistors (for monitoring and control)
- Heaters

## 2.1 PLM passive thermal control system

### 2.1.1 V-grooves

The V-Grooves (VG) system design is a key issue of the ARIEL thermal performance as they represent the first cooling stage of the PLM. VGs are high efficiency, passive radiant coolers, whose performances in a cold radiative environment such as L2 has been definitely demonstrated by the Planck mission [9]. The ARIEL V-Grooves system consists in a set of three specular shields working in sequence, composed by six semi-circular panels arranged in a “V-shaped” configuration, each one with a specific inclination with respect to the S/C X-Y plane (Fig. 5). Their objective is to intercept radiative and conductive heat leaks from warmer sections of the S/C and reject it to deep space after multiple reflections between each VG pair.

The VGs are light-weight sandwich panels with Aluminium 5056 alloy hexagonal honeycomb core (3/16–5056-0.0007) and Al 1085 0.25 mm thick external skins. Each VG shield is tilted by a certain angle with respect to the adjacent one, creating a divergent radiative path for the reflected thermal rays. Figure 5 shows a very simplified schematic of this concept. In the present baseline of the ARIEL PLM thermal configuration, the three VG angles are 7°-14°-21°. The three radiators are mechanically supported on the SVM interface by means of a total of 8 low conductivity struts. These struts are hollow tubes made of GFRP with Ti alloy (Ti6Al4V) end fittings.

The thermo-optical properties of the VGs are of essential importance since they are the key parameters for thermal isolation and heat rejection to space. To achieve the required performances, VGs surfaces must have a very low emittance coating, a high reflection/mirroring material needed to reflect thermal radiation. A Vapour Deposited Aluminium (VDA) layer can reach an emissivity in the IR band of less

than 0.05, as measured on the Planck PLM [9], with a specular reflectivity as high as 95%. The upper surface of VG3, exposed to the cold sky, is coated with high emissivity black paint (e.g. MAP PUK, or Aeroglaze Z306). It has been demonstrated experimentally that for this type of coatings the IR emissivity at cryogenic temperature can decrease by a factor of 2. For this reason, in order to maintain the required emissivity at low temperatures, the properties and performances of several possible solutions to increase the emissivity of coatings at low temperatures are under investigation. As the VG3 heat rejection capability is key to the whole PLM thermal performances, in order to maximize the radiative coupling to deep space at low temperatures, a black painted open aluminium honeycomb configuration is baselined. The Planck mission has demonstrated that this solution is able to maintain the surfaces IR emissivity well above the required value,  $\epsilon > 0.8$ .

The harness from the warm electronics in the SVM to the cold units should be thermally coupled to each VG in order to reject its conductive load and minimize the leak to the coldest stages. In the present baseline configuration, as already reported, this is true only for the thermal and M2M control harness as the detectors control cables exchange heat only with the first V-Groove and not with the other two. This solution is required to maintain the channels SIDECAR above their safe operating temperature.

The JT cooler piping dissipates the gas pre-cooling load on the V-Grooves by means of a heat exchanger located on each stage. The assumed loads on the three V-Grooves for thermal analysis purposes are, at this stage, 65–180, 20–120 and 40–140 mW (Cold – Hot Case), respectively for VG1, VG2 and VG3. In these conditions, the present VG thermal design is sufficient to limit the temperature gradient over the shields to less than 3 K between the hot spots (cooler & harness heat exchangers) and the rest of the panel. The actual precooling loads depend on the required mass flow and on the VGs temperature. For this reason, a more realistic assumption, based on analytical fit functions, will be integrated in the payload Thermal Mathematical Model (TMM) in the next phase.

### 2.1.2 Bipods

The bipods (Fig. 6) are hollow tubes made of low conductivity material. At this stage, CFRP is baselined as the tubes material with a diameter of 48 mm and 2 mm wall thickness. Ti alloy (Ti6Al4V) end fittings connect them to the Aluminium alloy feet and heads. The rear and front bipods leg length is respectively ~625 mm and ~400 mm.

The main task of the bipods design is to maximise the mechanical support and performances of the whole Telescope Assembly while limiting the thermal conductance across the stages. Each bipod leg tube is filled with rigid foam (or IR filters at various temperature stages) to avoid internal reflections, minimizing any possible radiative coupling between the warm and cold ends. During flight operations they will always face the cold sky so their external surface shall be black painted to maximize heat rejection to space. This configuration ensures a very limited heat leak to the TOB across the full length of the bipods (on the order of few mW).

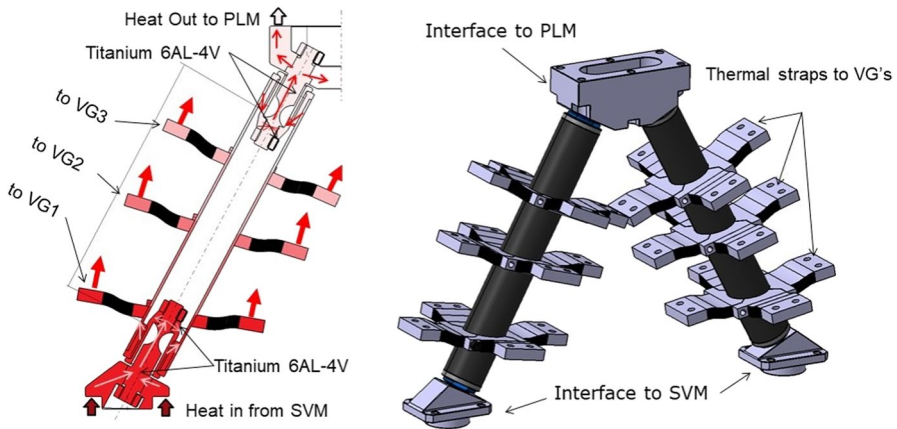


**Fig. 6** Bipods configuration

The bipods, as well as the VG struts, must be thermally coupled to the V-Grooves, to minimize heat leaks to the PLM colder stages. Each bipod leg is connected to each VG by means of thermal straps, as shown in Fig. 6.

### 2.1.3 Telescope baffle and instrument radiator

The V-Groove-based design provides a cold and stable environment for the telescope, instruments and cryocooler cold end. In this cold volume all main surfaces exposed to space work as radiating units to increase performances and margins of the PLM passive design. The two main surfaces operating as passive stage reference for the instrument and the telescope are the Instrument Radiator and the top half of the Telescope Baffle. The exposed areas of the Optical Bench can also help in this direction, providing an extra heat rejection surface.

The baseline thermo-optical design of the external surfaces is based on high IR emissivity coatings (black paint, such as MAP PUK or Aeroglaze Z306, with  $\epsilon_{IR} \geq 0.9$  at room temperature) to maximize radiative coupling to cold space. As already mentioned, further studies are in progress to investigate the expected behaviour of the IR coatings at cryogenic temperatures and to evaluate possible solutions for an improved emissivity. For this reason, at this stage, it is assumed that the thermo-optical design of the Instrument Radiator external surface is based on a black painted open honeycomb structure. The internal surface of the Baffle, the TOB and the Instrument Radiator, facing the telescope and the instrument cavity, is black painted also for stray-light control purposes.

At present, the Instrument Radiator is mounted directly on the TOB and operates as a lid for the Instrument Cavity, bolted to the bench. Its function is to operate as an efficient radiating surface to help maintaining the temperature of the TOB and the units on it in their operating range.

In the present thermal configuration, the radiator is able to operate at temperatures in the 50 – 60 K range while rejecting up to 200 mW to deep space. At present, the Instrument Radiator approximated top face area is around 0.4 m<sup>2</sup>. In case a larger margin is required, a wider surface (in the 0.4–0.5 m<sup>2</sup> range) could be easily fit on top of the allocated volume on the optical bench, if the relative mass increase can be allowed in the budget. The radiator orientation is parallel to the TOB with an angle around 7° with respect to the vertical direction.

If needed, in the next design phase of the project, the Radiator can be used either to provide a stable reference for the FGS detectors (now directly mounted on the module box), to reject the cryo-harness heat leak (now dissipated on the TOB) or to dissipate the heat load due to the discrete CFEE of the AIRS module. In all cases, the Radiator shall be thermally decoupled from the TOB to minimize the impact on the TOB temperature and stability.

At present the Baffle is designed as a simple black painted shroud made of a 2 mm Al6061 alloy layer. This thermo-mechanical configuration reduces mass while ensuring at the same time a good thermal conductance and mechanical stiffness. The baffle is mechanically supported on the optical bench and on the two stiffening arms of the telescope structure by brackets that minimize any possible stress to the telescope structure due to thermo-elastic effects. The thermal analysis results show that using the top half of the Telescope Baffle as an extra PLM radiator, given its large surface, offers a great chance of improving the passive thermal performances of the mission. For this reason, the baffle is also thermally connected with high conductance straps to the Optical Bench to operate as a single large passive stage (TIF4) for all instrument units.

### 2.1.4 Thermal straps

The main conductive links of the ARIEL PLM units are based on high purity 5 N Al braids (wires or foils). Because of the high thermal conductivity of pure Al in the 40–60 K range (around 1000 W/m-K) and its low density, it is possible to maintain dimensions, and mass, of the braids within allocations. The straps are used to thermally connect:

- the bipods to the VGs for conductive parasitic leaks interception: at least one straps per bipod leg per VG;
- the Telescope Baffle to the Optical Bench (four straps);
- the instruments' FPAs to their temperature reference (radiator or cooler cold end): one per detector assembly.

At this stage, in the thermal analysis, the straps are simulated by dedicated conductors that simulate the total conductance across each strap. This conductance evaluation includes: the combination in series of the conductance through the flanges and braids and the contact conductance at the interfaces, plus some efficiency factors that take into account realistic inefficiencies in the density of wires (or foils) per

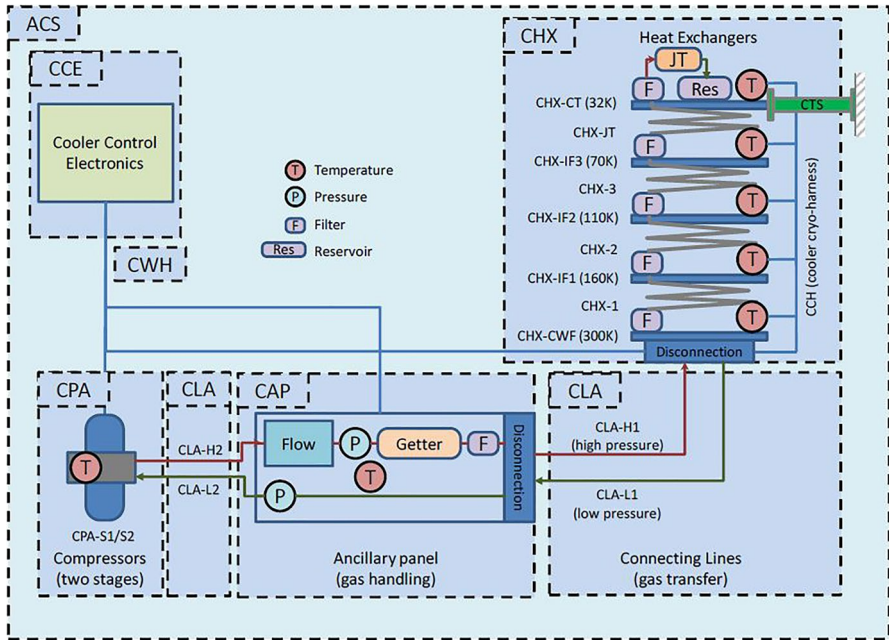


Fig. 7 ACS JT cooler schematic

unit area, in the effective length of the link (due to turn and bends) and in the welds of the braids to the end flanges.

## 2.2 PLM active thermal control system

### 2.2.1 Neon JT active cooling system

The Active Cooling System (ACS) is being used to cool both channels of the Ariel Infra-Red Spectrometer (AIRS) detector focal planes to a temperature of 42 K or below. The ACS is a closed cycle Joule-Thomson (JT) mechanical cryocooler using Neon as the working fluid. A schematic of the ACS is shown in Fig. 7.

The ACS provides active cooling at the cold tip thermal interface by performing a Joule-Thomson expansion of the working fluid across a restriction, in this case an orifice. The cooler is operated sub-critical, collecting the liquid produced after expansion in a reservoir such that the heat exchanger return-line pressure above this reservoir determines the temperature. The cooling power achieved depends upon the fluid mass-flow through the orifice as well as the initial and final states of the fluid before and after the expansion process. In general, greatest cooling occurs when the fluid is initially pre-cooled well below its inversion temperature, with its initial pressure close to the inversion curve boundary and its final pressure much lower.

The cooler is required to provide 88 mW (including margins) of cooling at a temperature of  $\leq 35.0$  K in order for the AIRS detectors to operate at  $< 42$  K. Neon is

selected as the working fluid because its boiling point (27.05 K at 1 atm) is well matched to the temperature requirement. In nominal operation the return line pressure is designed to work at  $\sim 3.5$  bar which gives a cold tip temperature of  $\sim 32$  K, and the inlet line pressure is designed to be around 20 bar, which is very much lower than the inversion curve boundary ( $\sim 300$  bar at 100 K), but is accessible for reciprocating compressors.

The compressors (CPA) circulate the Ne gas around the system by a set of reciprocating linear motor compression stages, with an arrangement of reed valves and buffer volumes, to produce a DC flow through the Joule-Thomson orifice whilst maintaining the pressure ratio across it. Two compression stages in series (CPA-S1 and CPA-S2) are needed in order to produce the required high and low pressures.

The gas must be pre-cooled prior to the Joule-Thomson expansion taking place, there are three pre-cooling stages available from the spacecraft V-Groove radiators and, to reduce the heat rejected at these pre-cooling interfaces (CHX-IFn), counter-flow heat exchangers (CHX-n) are used between them.

The ancillary panel (CAP) carries gas handling and measuring equipment, as well as particulate filters and a reactive getter to ensure gas cleanliness, which is critical to the long term operation of the cooler. The disconnection plates and connecting pipework (CLA) allow the system to be separated into several pieces to aid integration. This allows the heat exchanger assembly to be delivered and integrated with an instrument independently from the CPA and CAP, with a final purge and gas fill procedure being carried out after installation of the CLA to re-connect the CPA/CAP to the CHX.

The cooler is controlled by a set of drive electronics, housed in the Cryocooler Control Electronics (CCE) unit, which perform all commanding and controlling functions as well as providing the electrical input power for the compressors and returning the cooler housekeeping data.

The cooling power as a function of high pressure and mass-flow is shown in Fig. 8.

Several operating points satisfying the cooling power requirement (88.0 mW plus 20% margin) have been identified for the ACS. A range of combinations of these operating parameters is given in the table below: the nominal operating configuration (high-lighted) is selected on the basis of a trade-off between cooler parameters on one side and precooling stages dissipation on the other, as the ACS must be compliant with maximum heat rejection allocations for the full range of the V-Grooves temperatures (Table 2).

### 2.2.2 Thermal monitoring: Thermistors

The knowledge of the payload units' thermal conditions during flight operations is a key issue for the evaluation of the mission technical and scientific performances. A detailed temperature monitoring is achieved by the combination of direct measurements with thermal analysis results, correlated with all ground test data at sub-system and system level. For the instruments units and the cooler cold end monitoring, Cernox thermistors are the baseline. For the telescope and other PLM passive units (such as the V-Grooves) diodes sensors can be used, using Cernox only for critical interfaces or thermal control purposes.

**Fig. 8** ACS cooling power as a function of high pressure and mass flow at 32 K with worst case 67 K precooling temperature

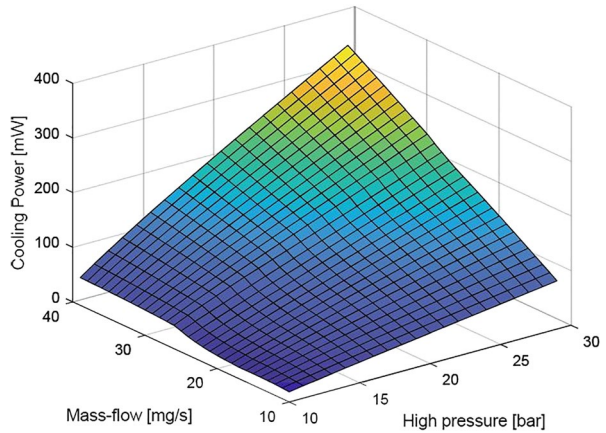


**Table 2.** Heat exchanger performance for a range of operating points satisfying the cooling requirement.

| High pressure [bar] | Mass flow [mg/s] | Heat rejected to 1st stage [mW] | Heat rejected to 2nd stage [mW] | Heat rejected to 3rd stage [mW] | Pressure drop in LP line [mbar] | Cooling power [mW] |
|---------------------|------------------|---------------------------------|---------------------------------|---------------------------------|---------------------------------|--------------------|
| 15                  | 29.0             | 129                             | 46                              | 161                             | 63                              | 105.5              |
| 20                  | 19.8             | 101                             | 45                              | 99                              | 45                              | 105.4              |
| 25                  | 14.3             | 84                              | 40                              | 78                              | 34                              | 105.4              |

The total number of sensors needed to monitor the PLM is still under definition. The present estimation is around 40 fully redundant thermistors. This number must be kept as low as possible in order to minimize the number of wires and the read-out electronics complexity. At the same time the thermistors shall be enough to ensure, in combination to the thermal maps resulting from the correlated TMM, a complete monitoring of the PLM during flight operations. A thermistor is installed in correspondence of each unit’s TRP, main thermal interface or critical item. At this stage, all thermistors are assumed to be fully redundant. The thermometers inside each module box, for detector, CFEE or optical units’ thermal control are monitored by the associated DCU. The JT cooler sensors are read by the cooler electronics. All other PLM thermistors are read and acquired by the TCU.

The reading/acquisition rate of the temperature of critical items (such as the instrument radiator or the optical bench) shall be 1 Hz. The other passive units (such as the V-Grooves or the Baffle) can be monitored at a relaxed rate (with periods of tens of seconds), especially if they are dominated by low frequency variations. All thermistors read-out is based on 4-wires measurement with connections to the read-out electronics arranged in shielded twisted pairs to minimize EMI from external sources. A resolution of at least 25 mK and an accuracy of 50 mK are required for the units on the TOB, for the Instrument Radiator and for the Primary Mirror when they are in their operational range. The thermistors used for thermal control should



have a resolution of at least 10 mK for the detectors and 25 mK for the M1 in the operating temperature range.

### 2.2.3 Thermal control: Heating lines

Stable conditions during observations are a key requirement for the scientific objectives of ARIEL. For this reason, thermal stability is one of the key drivers of the mission design. There are several possible thermal noise sources in the PLM: electrical dissipations instabilities, due to changes in the operating processes or modes, radiator temperature oscillations and cooler cold end fluctuations. The main cause of thermal fluctuations on radiators is due to attitude changes associated to the mission observation strategy, when repointing between two targets observations (on timescales of 10 h or so), or to seasonal variations (typically on longer periods like weeks, months, years). Experience on previous missions [9], testing and simulations show that low frequency oscillations due to active loads variations or to cryocooler instabilities, over a timescale of 10 h, can be controlled down to a level such that the thermal background stability does not represent a major contributor to the instrument noise budget. The most significant temperature variation will happen when the Sun aspect angle changes while repointing the S/C to observe a new science target. The SAA changes may cause variations of the temperature of the SVM radiators or of the PIP interface. The warm units' radiator changes could introduce thermal instabilities transmitted throughout the read-out chain either by changes in the parasitic fluxes or due to the electronics thermal susceptibility properties. Constraints on the maximum slew angle between successive targets are set to limit the SAA changes and the induced temperature variation to less than 10 K in the SVM top floor. This variation is further damped by more than 2 orders of magnitude at the PLM level, well below the temperature stability requirement as demonstrated by analysis and simulations. As a result, it is not anticipated that significant temperature regulation is needed for the units inside the SVM beyond the nominal regulation to keep the units in their allowed operating range.

In a JT cooler, instabilities at the reference heat exchanger temperature are due to compressor modulation, with its typical high frequency spectrum (30–40 Hz range), to cold-end internal mass flow 1- or 2-phase dynamics (on the order of tens of seconds) and to precooling stage variations (low frequency).

Thermal stability of the optical modules directly connected to the optical bench is not expected to be a major concern given the typical instabilities of passive radiators in L2 either on the timescales of the ARIEL detectors average exposure or of the seasonal variations. The high thermal inertia of the instrument bench and modules can damp the typical fluctuations of both timescales well below the requirement.

On the basis of the present knowledge of the possible thermal fluctuation sources in the ARIEL spacecraft, the telescope passive control design is more than enough to keep the M1 well below the required stability. A 10 K over 10 h' linear variation at SVM level induces a change of less than a mK on the M1 against a 2 K peak-to-peak requirement (see Chapter on the model results). At present, the thermal analysis indicates that there is no need of an active temperature control system for the primary mirror.

For all these reasons, the present baseline for PLM active thermal control is limited to survival and decontamination heaters. The design and implementation of the Decontamination and Survival Lines is under Consortium responsibility but they are operated by the S/C, as their activation must be triggered by operational phases, modes and conditions in which the PLM electronics is not operational.

The Decontamination Lines are activated in the cool down phase during transfer to L2 (first few weeks of flight). For decontamination purposes the temperature of the telescope mirrors, the TOB and the Instrument Radiator should be kept around or above 170 K (TBC), for approximately the first two weeks of flight operations. With the present thermo-mechanical design, the TMM prediction for the telescope mirrors and optical bench max decontamination power is around 170 W (with a 50% margin). Approximately 50 W are needed to take M1 temperature to 170 K once the mirror is already operating at 50 K, in case a decontamination run is needed during cold operations. The control logic for decontamination is based on a simple proportional loop.

The present baseline solution is to integrate the decontamination heaters directly on the back surface of the Al 6061 mirror as the possibility of integration on a radiative SLI panel behind the mirror to avoid direct contact does not seem a viable option due to mass (and power) allocation. In any case, the best solution will be analysed and evaluated in Phase B2. For this reason, the current baseline for the M1 decontamination heaters is to install them on the three whiffletree mountings to minimize stresses on the mirror during the cooldown phase. The use of Kapton film heaters glued and/or taped is preferred due to the better heat distribution and lower mass. Film heaters are widely used for cryogenic applications and a search for space qualified solutions related to their use on Al alloys will be carried out in the next phase of the project. In case no technical solution will be identified, a qualification campaign may be started within the TA development or the use of cartridge/Al cased heaters, bolted to the mirror mountings, can be evaluated as a possible solution. Another possibility is to use the TOB as a heating stage for the M1. The feasibility of this solution in terms of power allocation, efficiency and mirror response time will also be investigated in the next phase.

The Survival Lines are required to ensure that the Instrument CFEEs temperature does not fall, in any Operational Mode, below their safe temperature limit, 130 K. The SIDECARs temperature during Routine Operations is ensured by their active load dissipated on the dedicated radiators and by their thermal configuration. Every time the SIDECARs load is deactivated, the survival heating lines must take over and supply the required power to keep the units safe. Two Nominal Survival lines (plus two Redundant) are required, each one capable of providing power in the 0–1 W range.

### 3 PLM geometrical and thermal model (GTMM) description

The GTMM is based on the CAD model of the PLM and represent the main units, surfaces and structures with the necessary level of resolution to verify compliance to the thermal requirements. Small geometries and details which are not relevant for thermal analysis purposes are not considered.

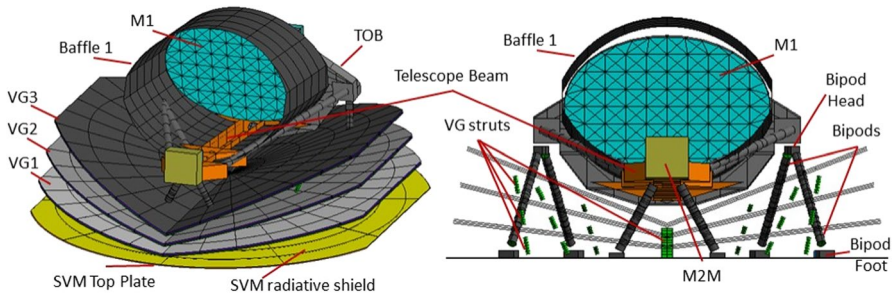


**Fig. 9** Front views of the PLM GMM with the SVM/PLM I/F

### 3.1 SVM/PLM Interface

In order to simulate the thermal coupling with the Service Module, the SVM to PLM interface platform is assumed as a boundary in the model. This SVM/PLM I/F is composed of two surfaces. The conductive one, called “SVM top plate”, operates in the 215–293 K temperature range and is the main interface of the bipods and V-Grooves struts. The second surface is the “SVM radiative shield”, located between the SVM top plate and the VG1, and represents a purely radiative shield, provided by a MLI blanket, coupling with the rest of the model. In the PLM thermal model, the SVM top plate interface is represented by two parallel discs, one for the SVM top plate and one simulating the SVM Radiative shield. Figure 9 shows front views of the entire model in ESATAN-TMS.

### 3.2 V-grooves

The V-Grooves (VGs) are represented as three couples of semi-circular panels with an inclination set of  $7^{\circ}$ – $14^{\circ}$ – $21^{\circ}$ . Each panel is modelled in detail in ESATAN-TMS in order to consider the different thermal properties of the external skins and the honeycomb core. Each VG semi-circle is composed of three identical shell geometries, representing the two skins and the honeycomb. A three dimensional conductivity vector is defined in the model to simulate the in-plane and the through thickness transverse heat flows of the honeycomb. All surfaces of the VGs are assumed as coated with VDA (Vapour Deposited Aluminium, emissivity  $\sim 0.045$ ) with the exception of the upper surface of the topmost VG which is covered by an open honeycomb layer with black coating to maximise the heat exchange with cold space.

The entire PLM passive cooling works only if the spacecraft cold section is shaded from the Sun once in orbit. The maximum allowed Solar Aspect Angle (SAA), with respect to the nominal attitude (Sun vector perpendicular to the SVM platform) is  $\pm 30^{\circ}$  along the  $\pm Y_{\text{ARIEL}}$  axis and  $\pm 11^{\circ}$  along the  $\pm X_{\text{ARIEL}}$  axis. This requirement, together with the dimensions of the SVM/PLM I/F, poses a limit on the maximum dimensions of the VGs. In order to have all three VGs inside the allowed envelope, it is necessary to cut VG1 and 2 at the  $\pm Y_{\text{ARIEL}}$  ends with a plane inclined by  $11^{\circ}$  from the SVM top plate. The third VG fits inside the shadowed envelope.

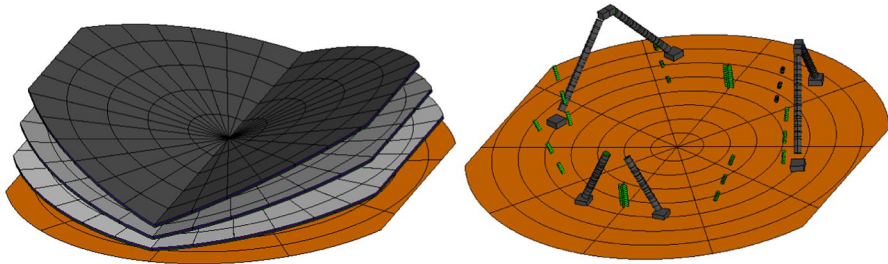


**Fig. 10** The three V-Grooves (left panel) and bipods plus supporting struts (green units in the right panel) connecting the SVM to upper and coldest parts of the PLM

### 3.3 Bipods and supporting struts

Three bipods and eight supporting struts connect the VG's, the OB and the telescope structure to the SVM top platform (Fig. 10, right). The bipods support the telescope structure and the Optical Bench (TOB). The struts are needed to support the V-Groove panels.

Bipod legs and VG supporting struts, made respectively of CFRP and GFRP, are modelled with hollow cylinder geometries. The bipods feet and heads are sketched as Al 6061 boxes, thermally linked to the legs with a conductance calculated assuming Ti6Al4V flexures with dimensions defined by the present CAD design. The bipods legs are filled with a special rigid foam (Eccostock SH is assumed on the basis of the Planck heritage) to avoid radiative coupling between the cold and warm sections of the tube internal surface. The foam thermal properties are assumed on the basis of the Planck measured values with enough margin to include uncertainties. The characteristics of the bipods and struts are summarized in Table 3. Dedicated links (user defined conductors) are used to model the straps that thermally connect the bipods to the V-Grooves for heat leaks interception.

### 3.4 Telescope: Mirrors, structures, baffle and telescope optical bench (Fig. 11)

In the G/TMM the telescope assembly is considered composed by the structure (Beam + Side Struts), the Baffle, the OB and the M1 and M2 mirrors. The M1 mirror (1100 mm × 750 mm) is simulated by a simplified geometry (see Fig. 13) while M2 is a simple disc shell. The bulk material of the mirrors is Al 6061 and their thermo-optical property is a very low emissivity surface, 0.02 (Silver is assumed), while the back is assumed as a machined Aluminium surface. The actual M1 maximum thickness is 200 mm but the mirror is not a full bulk of Al 6061. In the GTMM an average thickness of 72 mm is applied to the M1 shell geometry in order to account for the light-weighting cavities of the M1 back structure and to replicate a total mass of ~90 kg. The M1 is mechanically supported on the TOB by three triangular-shaped brackets (see Fig. 14). Each bracket is made of Al 6061 with an effective thickness of 30 mm. The blades are coupled to the bench by contact conductance while the thermal contact to the whiffle tree flanges and from these to the M1 is simulated by a set of user-defined conductors.

**Table 3** Bipods and V-Grooves supporting struts characteristics

| Structure                             | Dimensions | Thickness |
|---------------------------------------|------------|-----------|
| Front bipod (M2 side)                 | 48 mm Ø    | 2.0 mm    |
| Internal foam inside front bipod legs | 46 mm Ø    | NA        |
| Rear bipods (M1 side), × 2            | 48 mm Ø    | 2.0 mm    |
| Internal foam inside rear bipod legs  | 46 mm Ø    | NA        |
| VG Supporting struts, × 6             | 23 mm Ø    | 1.5 mm    |
| VG Central supporting struts, × 2     | 60x50x160  | 2.0       |

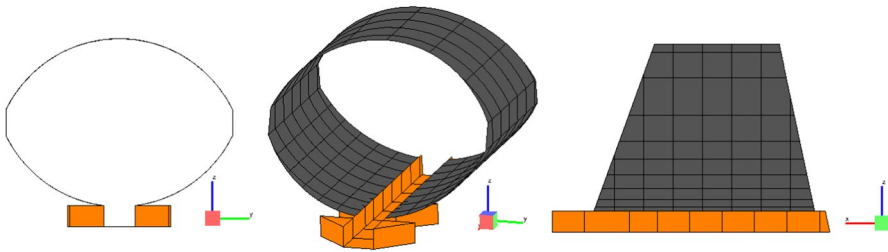


**Fig. 11** Three views of the Baffle M1 (dark grey) and the telescope beam (orange)

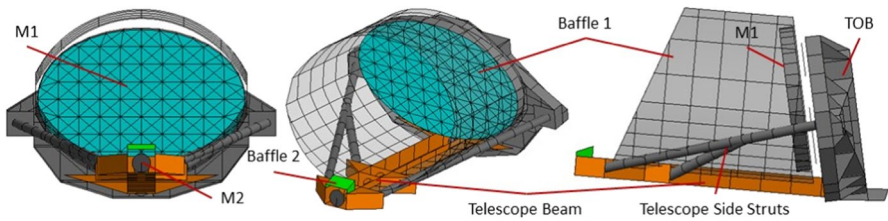
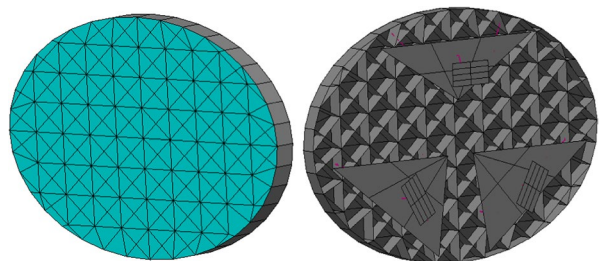


**Fig. 12** Three views of the Baffle, Telescope, TOB assembly. The Baffle is transparent to show the internal components

**Fig. 13** M1 GMM configuration



The M2 is placed at the end of the telescope beam. Behind it, the M2 re-focus mechanism is simulated by a box (see Fig. 9). The upper section of the M2 is shielded by a baffle (the M2 Baffle, the green shell in Fig. 12) used to avoid a direct

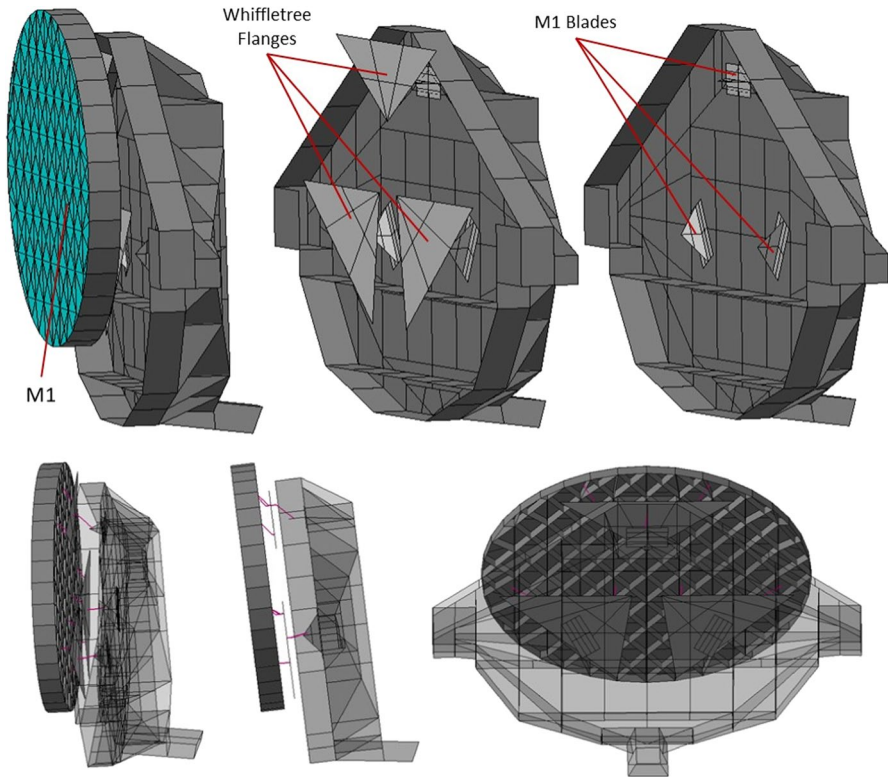


**Fig. 14** Top panel: views of the M1 mounting structure details in the GMM (blades and whiffle tree mountings). Bottom panel: M1 and TOB (transparent) showing the conductors linking the M1 blades to the Whiffletree brackets. The M1 blades are coupled to the TOB by means of a contact conductance

view of the sky by the M2. The secondary mirror, with its refocusing mechanism and baffle, is connected to the optical bench by the telescope beam. The beam is a U shaped structure composed of three rectangular shells. The beam, made of black painted Al 6061, shows four connecting flanges for the integration of the two stiffening arms that connect to the TOB. These arms are black painted hollow cylinders (made of Aluminium alloy) used to increase the rigidity of the whole Telescope Assembly. The front bipod is thermo-mechanically coupled to the two end flanges of the beam.

The Telescope Baffle structure is a composition of two circular cut cylindrical shells of the same radius vertically connected at their edges with two smaller rectangular surfaces (Fig. 11). The whole baffle structure has a front and a rear cut at, respectively,  $30^\circ$  and  $12^\circ$  with respect to the  $YZ_{\text{ARIEL}}$  plane, and another cut at rear-bottom to allow insertion of the bipods' interface with the TOB (Fig. 12). The Baffle is simulated as a 2 mm thick single shell of Al 6061. The thermo-optical design of the top half surface is assumed as a black painted panel to maximize the radiative coupling with the deep space on the outside and to minimize optical reflections in

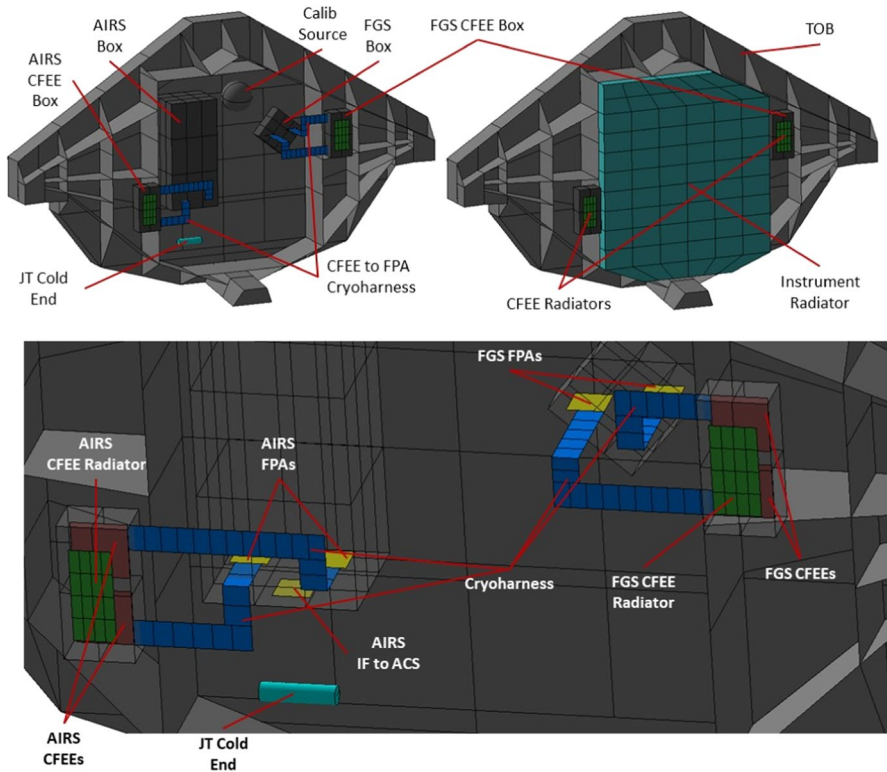


**Fig. 15** In the top part a general view of the TOB without and with the Instrument Radiator is shown. Below the Radiator there is the Instrument Cavity. The bottom left panel is a zoomed view, through transparent module boxes, of the components inside the TOB (the instrument radiator is hidden). The CFEs are coloured in red, the detectors in yellow, the JT cold end in cyan, the CFE radiators in green

the inner volume of the telescope. The Baffle is linked to the optical bench by six user-defined connectors with a conductance calculated on the basis of the brackets mechanical design.

The TOB shape and dimensions are based on the CAD design. The bench is sketched as a box composed by a series of triangular, rectangular and quadrilateral shells (see Fig. 15). The TOB is angled by  $7^\circ$  with respect to the  $YZ_{\text{ARIEL}}$  plane and located at the rear side of the Baffle. Each shell composing the TOB is Al 6061, 10 mm thick and coated with a black paint with IR emissivity  $\geq 0.6$  (IR diffuse reflectivity  $\leq 0.4$ ) at operating temperature.

### 3.5 Instrument assembly

The two instrument optical modules, FGS and AIRS, are located on the - X side of the telescope assembly, inside the TOB cavity (see Fig. 15). Both Cold Front End Electronics (CFEE) are mounted on dedicated radiators, sized to maintain the SIDECARs above their safe minimum temperature limit once the nominal load is

dissipated. Each instrument is modelled as a black painted Al 6061 box, containing the detectors and the channel common optics. The active JT cooler cold end interface is supported on the OB by an insulating strut just outside the AIRS box and is conductively linked to the two AIRS detectors by high conductance straps. The TOB cavity, with the modules, is closed by the Instrument Radiator that works as the cold temperature reference for the FGS detectors. In the baseline configuration each channel CFEE is coupled to a dedicated radiator. Both radiators area is approximately  $0.005 \text{ m}^2$  ( $\sim 5 \times 10 \text{ cm}$ ). This thermal accommodation of the CFEEs minimizes the distance between the CFEE and the FPA, keeping the harness length around approximately 25 cm, an acceptable value, while keeping the electronics well insulated above the cold optical bench.

### 3.6 Harness and cooler piping

In the present issue of the ARIEL PLM TMM the contribution of the harness and the cooler piping is evaluated by using defined conductors with an associated thermal conductance that simulate the present estimation of the heat leaks at each stage with a 50% margin. The harness for thermal and M2M control is assumed as split in two main branches both running from the SVM to the OB, dissipating on each V-Groove (see Fig. 16). The conductance of each branch in between all thermal stage is evaluated with the average of the heat loads calculated on the basis of the present level of design of harness and piping. The detectors control harness runs directly from VG1 to the CFEEs (each line with  $G = 0.0006 \text{ W/K}$ ) in order to help maintaining the SIDECARs temperature above the safety limit with an extra heat load.

The flexi-harness connecting the SIDECARs to the detectors is thermally coupled to the sides of the Optical Bench cavity with a  $G = 1 \text{ W/K}$  to minimize heat leaks from the CFEEs to the detectors. This is needed not only to minimize detectors T and load on reference stages (JT cold end and Instrument Radiator) but also to maximize electronics thermal insulation to maintain the safety temperature.

### 3.7 GTMM margins and uncertainties

In the present issue of the ARIEL PLM GTMM the margins assumed for the analyses presented are basically in line with the ESA document “Margin philosophy for science studies” [11]. The typical uncertainty assumed on the thermal analysis results was 10 K and 5 K on temperatures  $\geq 60 \text{ K}$  and  $< 60 \text{ K}$  respectively, with Acceptance and Qualification margins of 5 K each.

At present only a preliminary uncertainty analysis has been completed. Simulations have been run with the max and min values reported below to assess the main units’ sensitivity to each parameter:

- Metallic materials conductivity =  $\pm 15\%$
- GFRP/CFRP conductivity =  $\pm 30\%$
- Ti6Al4V conductivity =  $\pm 15\%$
- Contact conductance =  $\pm 50\%$



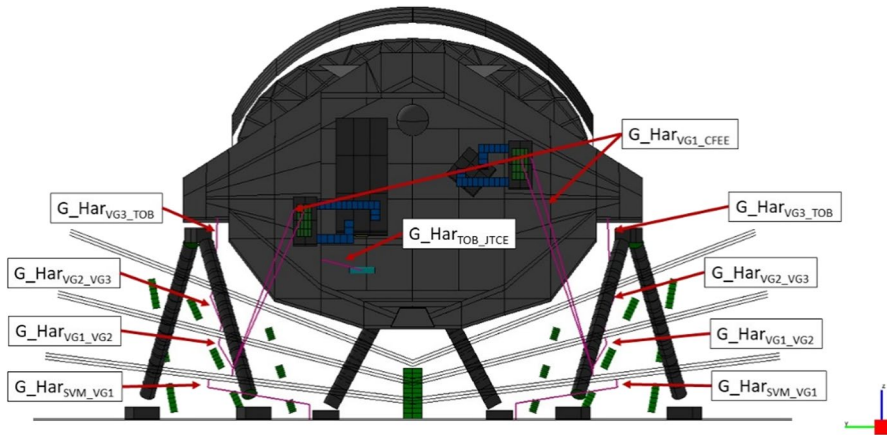


Fig. 16 PLM harness conductors' layout

- Black paint emissivity =  $\pm 10\%$
- SVM MLI emissivity =  $\pm 10\%$
- VDA emissivity (VG) =  $\pm 10\%$
- Hot case SVM IF temperature =  $\pm 10$  K (303 K conductive, 210 K radiative)

The analysis results show that the uncertainty is around 5 K on the VG stages and less than 3 K on the TOB, Telescope and Instruments temperature. With regard to the thermal analyses presented in this paper, these values are assumed to be already included in the margins taken on the results.

## 4 PLM thermal model results

### 4.1 Radiative case

To complete the description of the ARIEL PLM geometrical model, here are reported the radiative cases that have been run with the GMM. The radiative cases define how the model interacts with the orbit environment. The main orbital scenario assumed for the ARIEL PLM thermal analysis is the routine orbit around the Earth-Sun L2 point. This case is the radiative reference for the nominal orbit steady-state Hot and Cold TMM cases and for the time stability simulations: the PLM is placed at a circular Sun-centered orbit at  $1.5 \times 10^6$  km from the Sun, with the SVM plate perpendicular to the Sun vector (S/C Z axis in the Anti True Sun direction). The Sun illuminates the lower surface of the SVM top plate which totally shields the PLM from solar radiation. As described in the next section, in the present model assumptions the SVM top plate is simulated as a boundary node with assigned temperature conditions. Given the assumed radiative configuration, the PLM always results fully shaded from the Sun as far as the S/C attitude remains within the allowed SAA ( $\pm 11^\circ X_{\text{ARIEL}}$ ,  $\pm 30^\circ Y_{\text{ARIEL}}$ ). For this reason, no radiative case with varying SAA

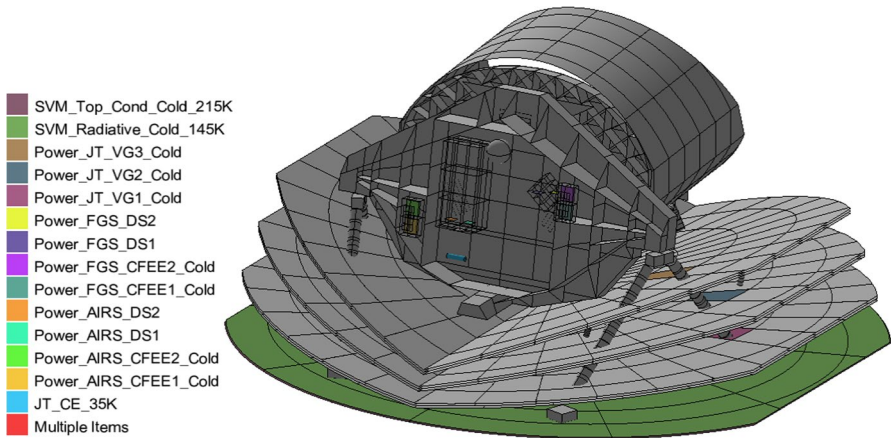


**Fig. 17** Boundary conditions (for the nominal cold case) associated to the corresponding nodes

has been computed at this stage. Once the SVM design will be in a more advanced state transient simulations of SAA changes will be carried out. In order to verify that the PLM geometry has been correctly simulated in the thermal model, all routine orbit cases have been run with the PLM tilted at the max SAA allowed:  $+11^\circ X_{\text{ARIEL}}$  and  $+30^\circ Y_{\text{ARIEL}}$ .

### 4.2 Boundary conditions and thermal cases

In order to fully characterize the PLM system thermal performance, different boundary conditions are considered. For each significant set of boundary conditions associated with a radiative scenario, a thermal-analysis case is created and solved. Table 4 and Fig. 17 report the power boundary conditions assumed for the nominal operation cases. The table includes the power dissipation of the instrument detectors and CFEEs and the precooling loads of the JT cooler. The power dissipation on VG1, VG2 and VG3 (last items in the table) refers to the power intercepted by the V-Grooves for pre-cooling the working fluid of the JT active cooler as per RAL worst case present estimation. The actual precooling loads depend on the required mass flow and on the VGs temperature. For this reason, a more realistic assumption, based on analytical fit functions that relate all these parameters together, will be integrated in the next issue of the TMM.

In all analysis cases of the TMM present issue, this heat load is totally allocated in one node of each V-Groove at the intersection of one of the rear bipod legs (the nodes are highlighted in colours in Fig. 17). This represents a worst case condition: this load is fully dissipated on the same V-Grooves node that intercepts the heat leak from the bipod. This configuration increases the power leaked to the optical bench.

The JT cooler cold tip is, at this stage, simulated as a boundary (perfect heat sink) at 35 K (worst case). This solution is used to evaluate the worst case incoming heat load and compare it to the heat lift capacity of the baseline cooler. On the other side, this assumption cannot represent the actual temperature behaviour of the cold tip

when loaded with variable heat fluxes. In the next issues of the PLM GTMM the JT cold tip will be more realistically simulated by a diffusion node with an associated analytical function to represent its temperature-dependent heat lift capacity. User defined conductors are used in the TMM to simulate the insulating strut supporting the cold end on the TOB.

The AIRS FPAs active load assumed for the thermal analysis (Table 4) is 2 mW (with margin). The TMM computes independently the heat leaks due to the struts and cryo-harness from the warm CFEE. The FGS configuration is the same but with an active load per detector focal plane of 20 mW.

Temperature boundary conditions are applied on both surfaces of the SVM/PLM I/F (conductive and radiative) to fully represent the thermal coupling of the PLM with the SVM in the present allowed range. All PLM nodes are represented as diffusion nodes. Table 5 reports the analysis cases presented in this paper with the associated radiative case and boundary conditions.

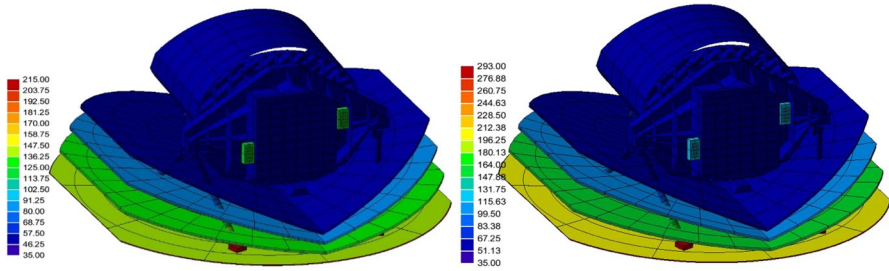
### 4.3 Nominal operations steady state thermal case: Cold and hot cases

Table 6 shows the solved steady-state temperatures of the cold and hot case for the nominal conditions, corresponding to the S/C orbiting at the Earth-Sun L2 point in routine operative, attitude and loads conditions. The main difference between the Cold and Hot Cases is given by the fixed boundary temperatures applied at the SVM/PLM I/F and by the respective estimated min and max precooling loads of the ACS.

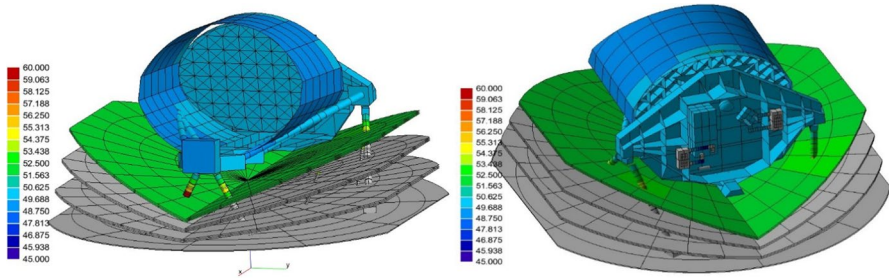
In the table below, the temperature results are compared to the requirements with the margins to be assumed at this stage of the design process. The margins described in Chapter 3.7 (see also Fig. 34 for a direct comparison with the analysis results) are not included in the values of the table. At present, as reported in Chapter 3.7, only a very preliminary uncertainty analysis has been performed: the uncertainty errors are, for the time being, assumed in the margin described. The temperature of all passively and actively cooled units are generally compliant to the requirements including margins. The unit temperatures maps for all cases are graphically shown in the next figures, comparing the Cold and Hot cases: general views of the PLM are compared in Fig. 18, 19, 20. Figure 21 to Fig. 26 compare the details of the main PLM units' temperature in both thermal cases (Table 6).

The V-Grooves and the TOB temperature results few to several degrees higher with respect to the past analyses. This is mainly due to the update of the bipods and of the feet dimensions, to the much higher cryo-harness loads (estimated at present as a worst case that shall be improved in the next project phase), to the reduced thermal performances of the Baffle as a radiating surface due the removal of the open honeycomb thermo-optical configuration and to the highest loads dissipated directly on the TOB (and not on the Instrument Radiator).

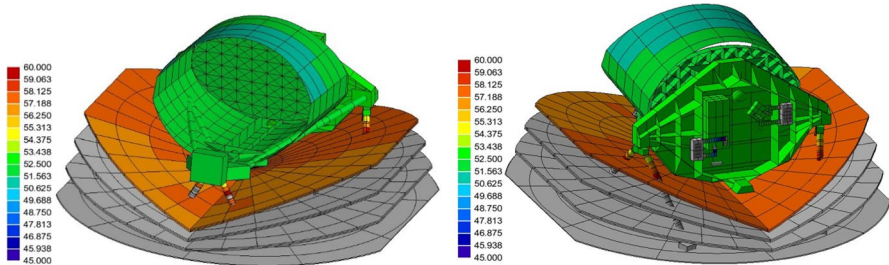
In Fig. 21 the optical bench temperature distribution in both thermal cases is shown: the max delta T across the optical bench is on the order of 200 mK in both thermal cases.



**Fig. 18** Cold Case (left panel) and Hot Case (right panel) PLM steady-state results in nominal conditions. Temperature is expressed in the absolute scale (K)



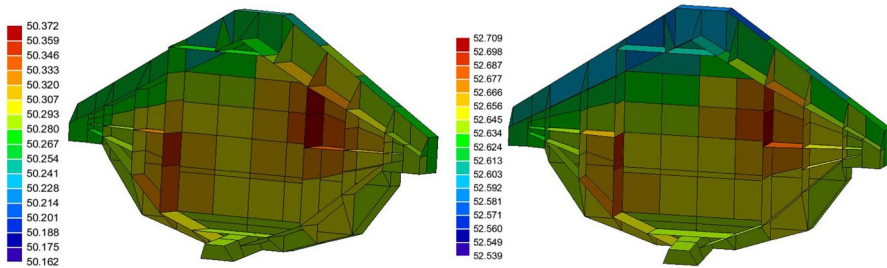
**Fig. 19** Cold Case steady-state results in nominal conditions in a narrower T range. Right side shows the radiator, OB, CFEE radiators and baffle temperatures. The radiator is hidden to show the module boxes on the Optical Bench. Temperature is expressed in the absolute scale (K)



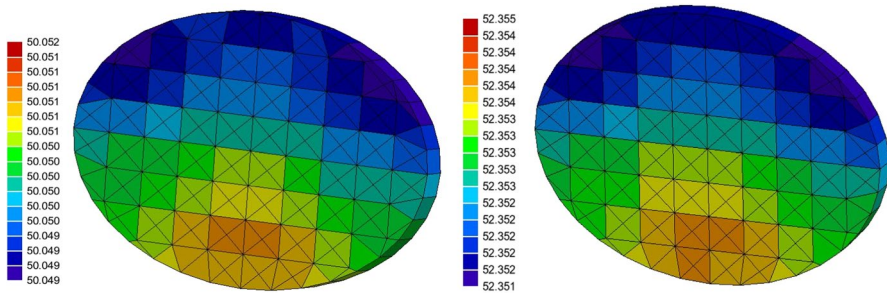
**Fig. 20** Hot case steady-state results in nominal conditions in a narrower T range. Right side shows the radiator, OB, CFEE radiators and baffle temperatures. The radiator is hidden to show the module boxes on the Optical Bench. Temperature is expressed in the absolute scale (K)

Figure 22 reports a more detailed view of the telescope primary mirror temperature distribution in both thermal cases, to show the thermal uniformity reached by the passive cooling. M1 maximum gradient is at the level of few mK: approximately 2.5 mK in the Cold Case and 3 mK in the Hot Case.

The temperature gradient across the V-Grooves in the two nominal cases is shown in the next Figures: VG1, VG2 and VG3, respectively in Fig. 23, Fig. 24, Fig. 25.



**Fig. 21** TOB temperature distribution. Cold case on the left and hot case on the right. Temperature is expressed in the absolute scale (K)



**Fig. 22** Telescope primary mirror T distribution in the Cold case (left) and the Hot Case (right). Temperature is expressed in the absolute scale (K)

The VG1 gradient is on the order of 3 to 5 K, while VG2 shows a delta T on the order of 1 degree or less.

The last V-Groove (VG3) is shown in Fig. 25: in both thermal cases the  $\Delta T$  across the whole surface is around 1 K if we include the hot spot (the node where most heat leaks are concentrated).

The temperature gradient across the bipods is shown in Fig. 26: in the Cold case the bipod legs withstand a total  $\Delta T$  of 165 K while in the Hot case the gradient is around 240 K. These large gradients require a bipod thermo-mechanical design with a very low total thermal conductance to minimize the parasitic heat leaks to the TOB. At the same time the bipods must have the mechanical properties needed to withstand the stresses and loads generated by the supported mass and by the thermal gradients. These requirements confirm that a composite material such as CFRP is the best candidates for a successful design.

The G/TMM performances in terms of heat fluxes to/from the PLM units and rejection capabilities of the passive cooling radiators are summarized in the following table (Table 7).

The table above provides an indication of the efficiency and performances of the ARIEL PLM passive design. The V-Groove 3 is capable of rejecting nearly 1 W at a temperature of 53 K (17 K below the requirement), while the telescope baffle and the instrument radiator dissipate to space, respectively, 0.39 W and 0.12 W at

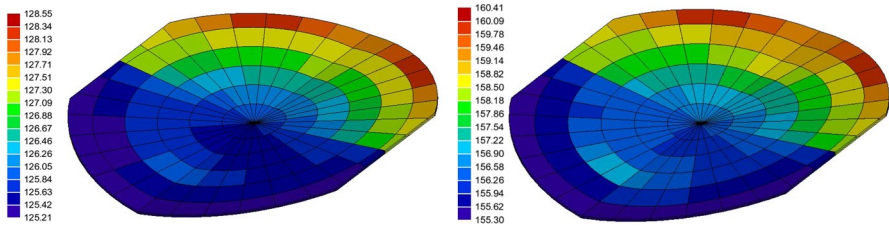


**Fig. 23** VG1 thermal gradient in the Cold (left) and Hot (right) cases. Temperature is expressed in the absolute scale (K)

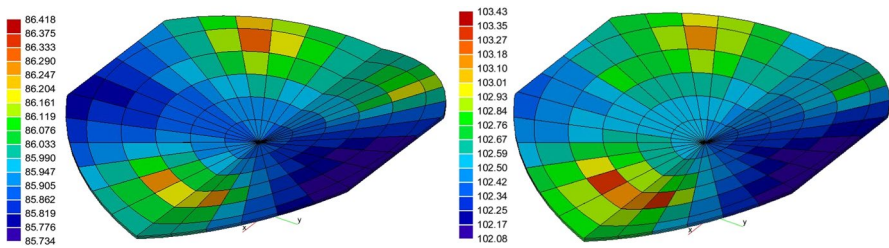


**Fig. 24** VG2 thermal gradient in the Cold (left) and Hot (right) cases. Temperature is expressed in the absolute scale (K)

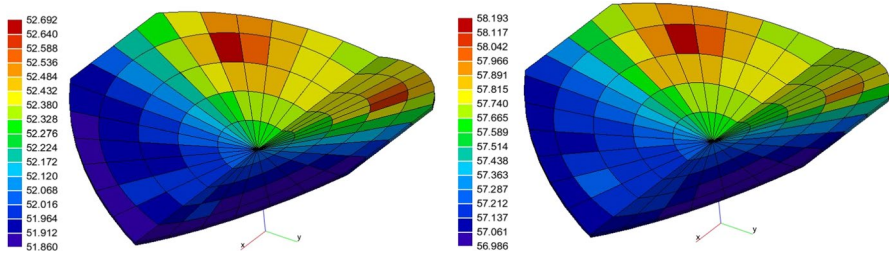


**Fig. 25** VG3 thermal gradient in the Cold (left) and Hot (right) cases. Temperature is expressed in the absolute scale (K)

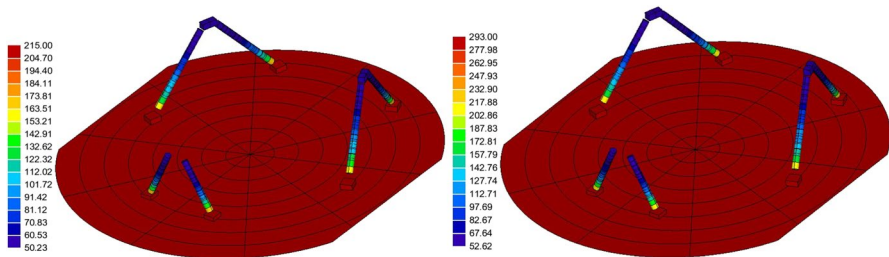


**Fig. 26** Bipods temperature distribution in the Cold (left) and Hot (right) cases. Temperature is expressed in the absolute scale (K)

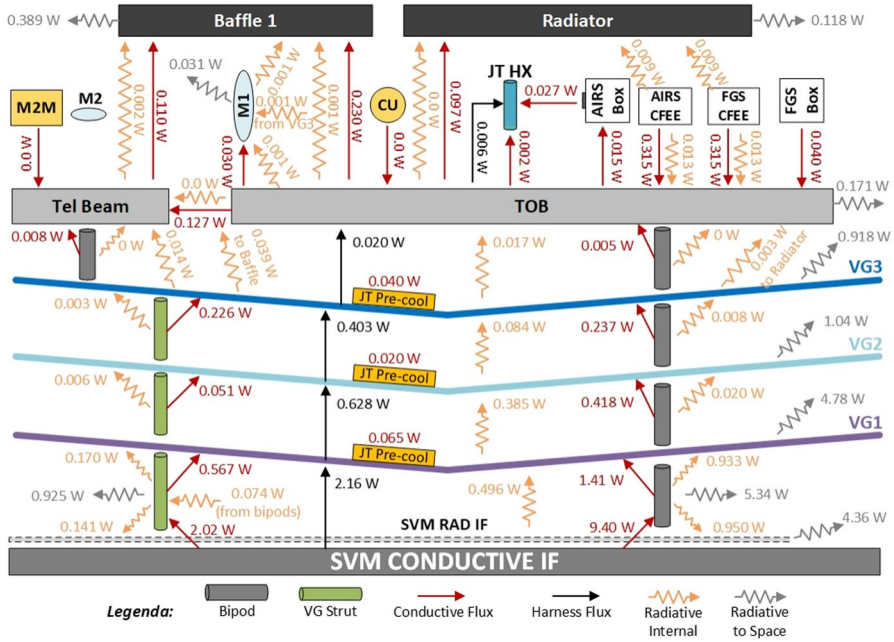


Fig. 27 Nominal Cold Case heat map

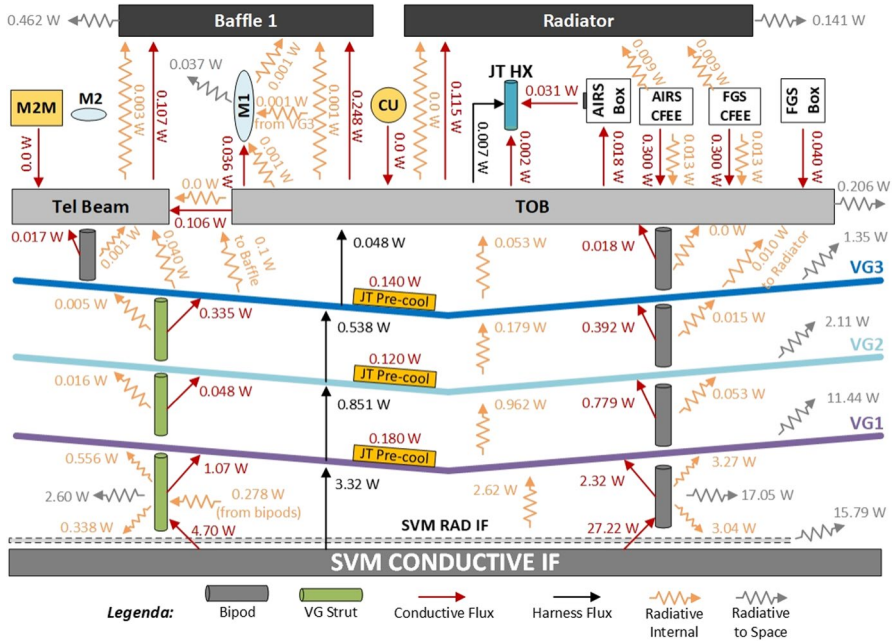
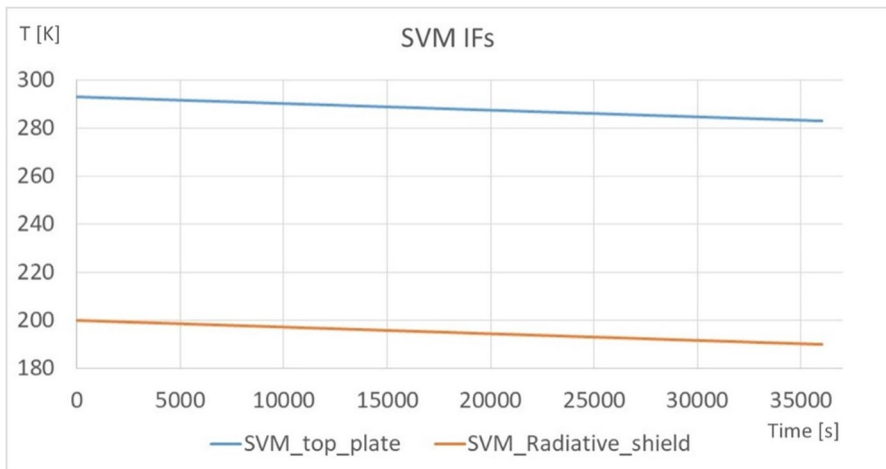


Fig. 28 Nominal Hot Case heat map



**Fig. 29** SVM IFs temperature time trend during the 10 h (36,000 s) period

temperatures well below the requirements. The details of the internal heat fluxes are summarized in the heat maps shown in the next two Figures (Figs. 27 and 28).

#### 4.4 Max instability case

Thermal stability is one of the key issue of the ARIEL PLM thermal design. The Max Instability case is run to verify the behaviour of the PLM with respect to the SVM Conductive and Radiative interfaces' temperature variation over time. The required max fluctuation of the SVM IFs during one observation run is 10 K over 10 h. The worst case fluctuations are the slowest ones, as they are not filtered out efficiently by the thermal capacitance of the PLM. For this reason, at this stage, it is assumed a slow but constant variation of 1 K/h over the 10 h' period. The SVM to PLM IFs variation is simulated by changing the boundary temperature of the SVM top plate and radiative shield during the transient solution routine: the SVM boundary temperatures change linearly from 293 K to 283 K (Conductive IF) and from 200 K to 190 K (Radiative IF) during the whole duration of 10 h of the transient process (1 K per hour) (Fig. 29).

The behaviour in time of the PLM main units is shown in the next Figures (Fig. 30).

As shown in the Figure above, most of the conducted temperature change is filtered out by the VGs and bipods sub-system. The transmitted effect on the TOB and Module boxes is on the order of 3 mK (Fig. 31 and 32).

The Telescope Mirrors show a different behaviour with time. The M1 temperature remains nearly constant, decreasing by 0.1 mK, due to the good level of thermal insulation and the high thermal capacitance. The Secondary Mirror, on the other side, is less insulated from the Telescope Metering Structure and can feel the influence of the shorter front bipod. For these reason, its temperature change is on the



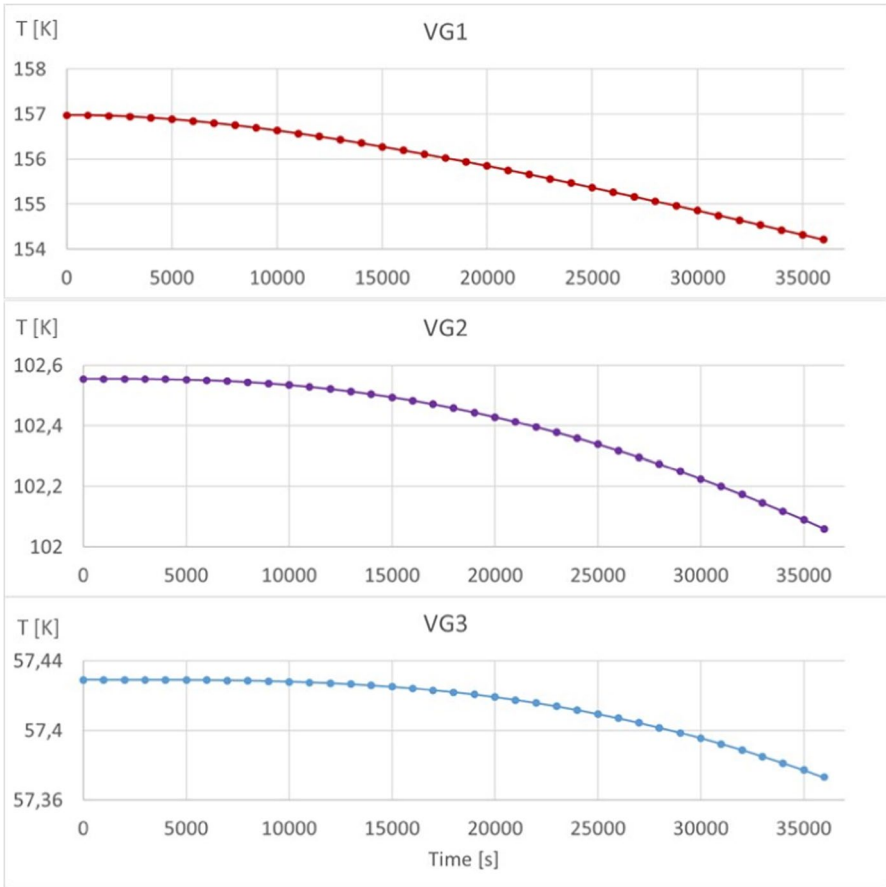


Fig. 30 V-Grooves temperature variation with time

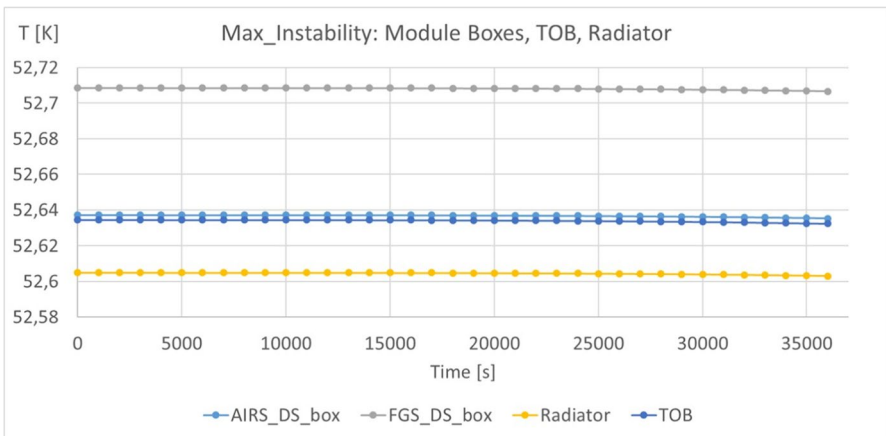


Fig. 31 TOB units' temperature variation with time

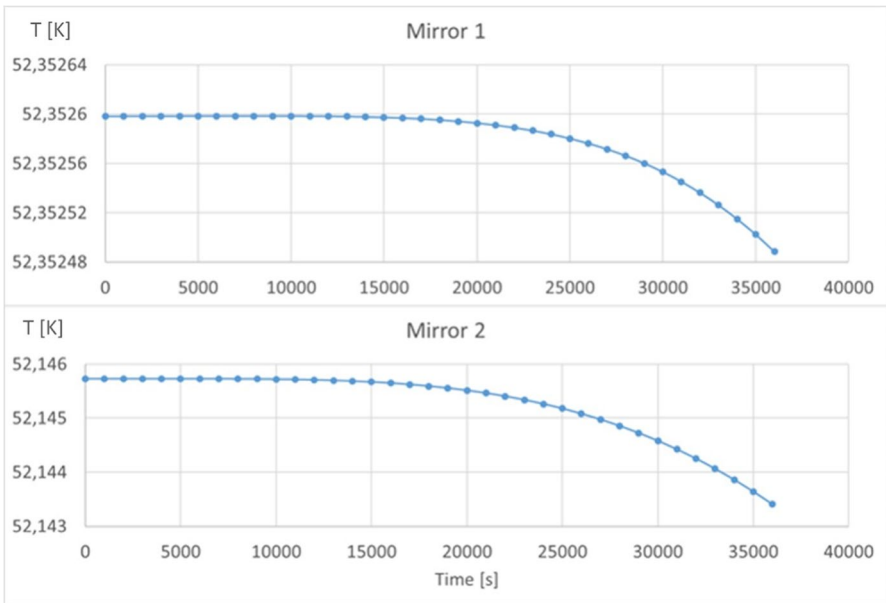


Fig. 32 Telescope mirrors temperature variation with time

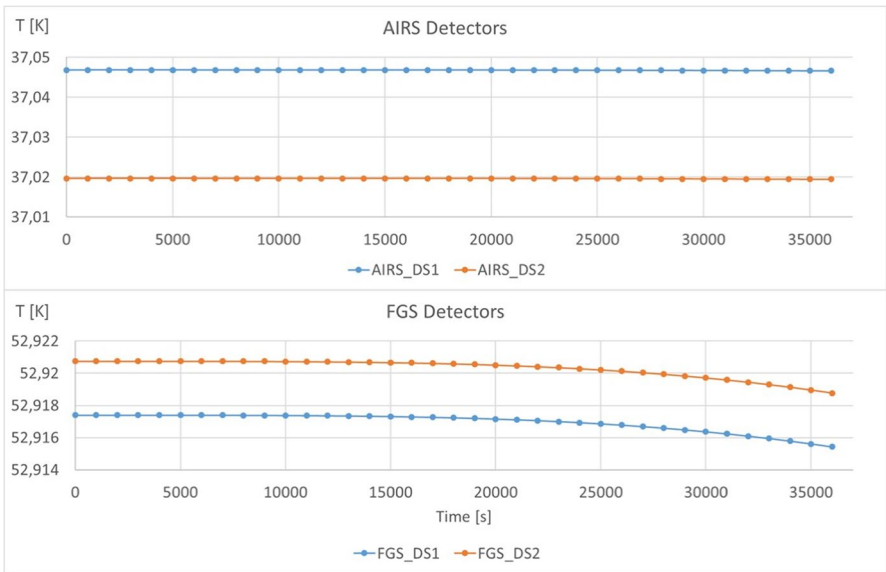


Fig. 33 Instrument detectors temperature variation

order of 2 mK. If deemed necessary, a better thermal insulation of the M2 mirror from the Telescope Beam and M2M, could be implemented (Fig. 33).

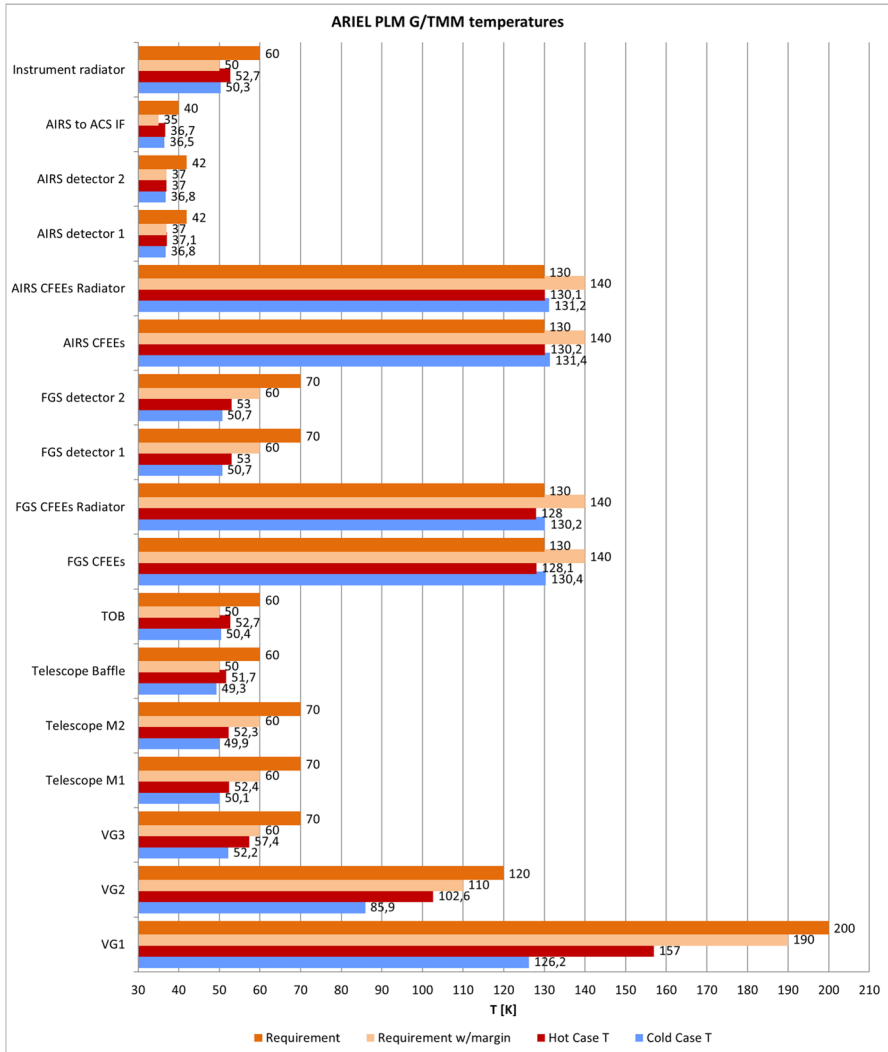


Fig. 34 Average temperature results of the PLM units

The detectors experience a different time trend: the temperature of the AIRS FPAs decreases by 0.2 mK while the FGS focal planes change by 3 mK due to their good thermal coupling to the Optical Bench.

In general, the GTMM shows the very good level of thermal insulation of the PLM units with respect to the SVM. The relative damping factor of temperature variations in time spans from 3.5 for the VG1, to  $10^2$  for VG3, and up to  $10^3$  to  $10^4$  for the coldest units.

**Table 4** Boundary heat loads at nominal operations

| Node                 | Load Cold Case[mW] | Load Hot Case [mW] |
|----------------------|--------------------|--------------------|
| AIRS detector 1      | 2                  | 2                  |
| AIRS detector 2      | 2                  | 2                  |
| FGS detector 1       | 20                 | 20                 |
| FGS detector 2       | 20                 | 20                 |
| AIRS CFEE 1          | 210                | 185                |
| AIRS CFEE 2          | 210                | 185                |
| FGS CFEE 1           | 215                | 185                |
| FGS CFEE 2           | 215                | 185                |
| VG1 precooling stage | 65                 | 180                |
| VG2 precooling stage | 20                 | 120                |
| VG3 precooling stage | 40                 | 140                |

## 5 Summary and conclusions

The ARIEL PLM thermal model results in terms of heat fluxes across the interfaces and unit temperatures, indicate a reliable PLM thermal architecture, compliant to the requirements including the present level of margin assumed. The next steps of the thermal analysis will be aimed at following the higher level of detail evolution of the PLM design, to optimize the design and decrease the margins assumed while preparing a more reliable assessment of the model uncertainties.

Figure 34 shows a comparison of the Cold to Hot case operating temperature ranges of the main PLM units with the required values plus the margins to be assumed at this stage of the design process. The temperature of all passively and actively cooled units are in general compliant to the requirements including margins, with the following exceptions:

- the AIRS and FGS CFEEs temperature in the Hot/Cold case, as the present design of the radiators is based on the full available area of the top surface of the CFEE box. This inconsistency can be easily solved by trimming the radiators surface until the requirement is met with margin (140 K);
- the Baffle, the TOB and the Instrument Radiator average temperatures in the Hot case show a slight non-conformance (between 2 and 3 K). This is mainly due to margins and conservative assumptions on the conducted heat fluxes (e.g. the cryo-harness) and on the passive cooling performances of the PLM. In the next phases of the project, it is expected that a more advanced design of the payload will allow to relax margins on thermo-optical properties, heat rejection capabilities and parasitic leaks. The PLM thermal design will then be optimized to recover the few degrees of this incompliance.

The impact of operating the CFEEs at 130 K is a ~ 10 K higher temperature on the FGS detectors and a higher load on the JT cold end for the AIRS case. The AIRS detectors temperature stabilize well within requirement by dissipating

**Table 5** Thermal analysis cases

| <i>Analysis case</i>            | <i>Radiative case</i>      | <i>Boundary conditions</i>   | <i>Type of solution</i> |
|---------------------------------|----------------------------|--|-------------------------|
| Cold case in nominal operations | Routine Earth-Sun L2 orbit | - SVM conductive platform @ 215 K (fixed)<br>- SVM radiative platform @ 145 K (fixed)<br>- Loads as per Table 4<br>- JT cold end as fixed boundary at 35 K   | Steady-state            |
| Hot case in nominal operations  | Routine Earth-Sun L2 orbit | - SVM conductive platform @ 293 K (fixed)<br>- SVM radiative platform @ 200 K (fixed)<br>- Loads as per Table 4<br>- JT cold end as fixed boundary at 35 K   | Steady-state            |
| Max Instability                 | Routine Earth-Sun L2 orbit | - Based on the Hot Case SVM boundaries (Conductive = 293 K, Radiative = 200 K)<br>- 10 K over 10 h SVM top plate fluctuation with a rate of 1 K per hour on both the full SVM Conductive and Radiative Top Plate IFs | Transient (10 h)        |

**Table 6** Steady-state temperatures for the cold and hot case in nominal conditions

| PLM Unit   | Cold case T [K] | Hot case T [K] | Req [K] |
|--|-----------------|----------------|---------|
| <i>SVM top plate (fixed boundary)</i>  | 215.0           | 293.0          | –       |
| <i>SVM Radiative shield (fixed boundary)</i>   | 145.0           | 200.0          | –       |
| VG1  | 126.2           | 157.0          | ≤ 200   |
| VG2  | 85.9            | 102.6          | ≤ 120   |
| VG3  | 52.2            | 57.4           | ≤ 70    |
| Telescope M1   | 50.1            | 52.4           | < 70    |
| Telescope M2   | 49.9            | 52.3           | < 70    |
| Telescope Baffle   | 49.3            | 51.7           | ≤ 60    |
| TOB  | 50.4            | 52.7           | ≤ 60    |
| FGS CFEEs  | 130.4           | 128.1          | > 130   |
| FGS CFEEs Radiator   | 130.2           | 128.0          | ≥ 130   |
| FGS detector 1   | 50.7            | 53.0           | ≤ 70    |
| FGS detector 2   | 50.7            | 53.0           | ≤ 70    |
| Figures 7,8 contains poor quality of text in image. Otherwise, please provide replacement figure file. | 131.4           | 130.2          | > 130   |
| AIRS CFEEs Radiator  | 131.2           | 130.1          | ≥ 130   |
| AIRS detector 1  | 36.8            | 37.1           | ≤ 42    |
| AIRS detector 2  | 36.8            | 37.0           | ≤ 42    |
| AIRS IF to ACS   | 36.5            | 36.7           | ≤ 40    |
| Instrument radiator  | 50.3            | 52.7           | < 60    |
| <i>JT cold end (fixed boundary)</i>  | 35.0            | 35.0           | < 40    |

**Table 7** Heat exchange at the main internal interfaces and between units for Cold and Hot cases in nominal conditions

| PLM IF main heat flux                          | Cold case [W]      | Hot case [W]       |
|--|--------------------|--------------------|
| SVM conductive heat load to PLM                | 9.395              | 27.215             |
| SVM radiative heat load to PLM                 | 0.496              | 2.616              |
| VG1 heat rejection to space                    | 4.776              | 11.438             |
| VG2 heat rejection to space                    | 1.041              | 2.111              |
| VG3 heat rejection to space                    | 0.918              | 1.348              |
| Telescope Baffle heat rejection to space       | 0.389              | 0.462              |
| Instrument radiator heat rejection to space    | 0.118              | 0.141              |
| Optical Bench heat rejection to space          | 0.171              | 0.206              |
| Conductive heat flux from bipods' heads to TOB | 0.005              | 0.018              |
| Conductive heat flux from bipod 1 to Tel Beam  | 0.008              | 0.017              |
| Conductive heat flux from TOB to Baffle        | 0.230              | 0.248              |
| AIRS CFEE radiator heat rejection to space     | 0.203              | 0.163              |
| FGS CFEE radiator heat rejection to space      | 0.197              | 0.152              |
| Heat flux from FGS Box to TOB                  | 0.040              | 0.040              |
| Heat flux from AIRS to JT cold end             | 0.035 <sup>1</sup> | 0.040 <sup>1</sup> |

<sup>1</sup>JT cold end boundary at 35 K

**Table 8** ARIEL external thermal interface budget

| External Interface | Location       | IF to     | Hot Case |                        |
|--------------------|----------------|-----------|----------|------------------------|
|                    |                |           | T [K]    | Load <sup>1</sup> [mW] |
| TIF0               | SVM Conductive | Bipods    | 293      | 27,215                 |
|                    |                | VG struts |          | 4,697                  |
|                    | SVM Radiative  | VG1       | 200      | 2616                   |
|                    |                | Space     |          | 15,785                 |

<sup>1</sup>Total load: sum of incoming conductors heat load into the PLM unit

a heat load fully compliant to the heat lift allocated by the JT cooler. The extra temperature margin available for the AIRS detectors could be used to relax the heat load requirement on the JT cold tip, if needed. The last V-Groove and the Instrument Radiator operate at a temperature around 52 K and 50 K in the Cold Case and around 57 K and 53 K in the Hot Case, rejecting to space up to more than 1 W and 140 mW respectively. The Telescope Baffle contributes to the PLM passive cooling by dissipating nearly 400 mW to space.

The ARIEL PLM loads, especially for what concerns detectors dissipation, mechanical supports, piping and harness leaks, have been evaluated on the basis of the present knowledge of the units' design and of the heritage from more advanced projects (MIRI, Planck, Euclid etc. [9, 10]). Conservative estimations have been assumed and verified by thermal analysis with the PLM G/TMM. The

**Table 9** ARIEL internal thermal interfaces budget

| Thermal Interface | Location            | IF to  | Req T [K] | Hot Case |                        | Load (50% margin) [mW] |
|-------------------|---------------------|--|-----------|----------|------------------------|------------------------|
|                   |                     |  |           | T [K]    | Load <sup>1</sup> [mW] |                        |
| TIF1              | V-Groove 1          | Heat leaks from SVM (harness, struts, piping, radiation)                         | ≤ 200     | 157.0    | 11,438                 | 17,157                 |
| TIF2              | V-Groove 2          | Heat leaks from warmer stages (harness, struts, piping, radiation)               | ≤ 120     | 102.6    | 2111                   | 3167                   |
| TIF3              | V-Groove 3          | Heat leaks from warmer stages (harness, struts, piping, radiation)+JT precooling | ≤ 70      | 57.4     | 1348                   | 2022                   |
| TIF4              | TOB                 | IOB, all channels FEE, parasitic leaks   | ≤ 60      | 52.7     | 206                    | 309                    |
| TIF5              | Instrument Radiator | FGS detectors + T control stage loads + parasitic leaks                          | ≤ 60      | 51.7     | 141                    | 212                    |
| TIF6              | JT cold end         | AIRS detectors + T control stage loads + full parasitic leaks                    | < 42      | 35       | 40                     | 60                     |
| TIF7              | CFEE radiators      | FGS SIDECARs   | > 130     | 128.0    | 315                    | 473                    |
|                   |                     | AIRS SIDECARs  | > 130     | 130.1    | 315                    | 473                    |

<sup>1</sup> Total load: sum of incoming conductors heat load into the PLM unit

budget resulting at the external interface and at the seven main internal interfaces from the analysis activity is reported in Table 8 and Table 9. The values correspond to the loads calculated by the TMM in the worst Hot reference case. The fact that the heat fluxes reported in Table 9 correspond to interface temperatures lower than required, indicate that extra margin is available for optimizations in the next phase.

**Availability of data and material** At present, the data of the thermal analysis are available to the ARIEL Consortium and ESA Team members only.

**Code availability (software application or custom code)** The work presented in this paper has been carried out by using commercially available software.

**Funding** Open access funding provided by INAF - National Institute for Astrophysics within the CRUI-CARE Agreement. This activity has been realized under the Italian Space Agency (ASI) contract with the National Institute for Astrophysics (INAF) n. 2018–22-HH.0.

## Declarations

**Conflicts of interest/competing interests** The authors declare no conflict of interest.

**Open Access** This article is licensed under a Creative Commons Attribution 4.0 International License, which permits use, sharing, adaptation, distribution and reproduction in any medium or format, as long as you give appropriate credit to the original author(s) and the source, provide a link to the Creative Commons licence, and indicate if changes were made. The images or other third party material in this article are included in the article's Creative Commons licence, unless indicated otherwise in a credit line to the material. If material is not included in the article's Creative Commons licence and your intended use is not permitted by statutory regulation or exceeds the permitted use, you will need to obtain permission directly from the copyright holder. To view a copy of this licence, visit <http://creativecommons.org/licenses/by/4.0/>.

## References


1. Tinetti, G., et al.: A chemical survey of exoplanets with ARIEL. *Exp. Astron.* **46**, 135–209 (2018)
2. Turrini, D., et al.: The contribution of the ARIEL space mission to the study of planetary formation. *Exp. Astron.* **46**, 45–65 (2018)
3. Puig, L., et al.: The phase a study of the ESA M4 mission candidate ARIEL. *Exp. Astron.* **46**, 211–239 (2018)
4. Pascale, E., et al.: “The ARIEL space mission”, space telescopes and instrumentation 2018: optical, Infrared, and millimeter wave. *Proc of SPIE.* **10698**, 106980H (2018)
5. Middleton, K.F.: “An integrated payload design for the atmospheric remote-sensing Infrared exoplanet large-survey (ARIEL): results from phase a and forward look to phase B1”, international conference on space optics — ICSO 2018. *Proc. of SPIE Vol.* **11180**, 1118036 (2018)
6. Da Deppo, V., et al.: “The optical configuration of the telescope for the ARIEL ESA mission”, space telescopes and instrumentation 2018: optical, Infrared, and millimeter wave. *Proc. SPIE.* **10698**, 106984O (2018)
7. Rataj, M., et al.: “Design of fine guidance system (FGS) for ARIEL mission”, photonics applications in astronomy, communications, industry, and high-energy physics experiments 2019. *Proc. Of SPIE Vol. Proc. SPIE.* **11176**, 111763E (2019)
8. Focardi, M., et al.: The ARIEL instrument control unit design. *Exp. Astron.* **46**, pages1–30 (2018)
9. Planck collaboration: Planck early results. II. The thermal performance of Planck. *Astronomy & Astrophysics.* **536**, A2 (2011)



10. B. M. Shaughnessy and P. Eccleston. "Thermal Design of the Mid-Infrared Instrument (MIRI) for the James Webb Space Telescope". International Conference on Environmental Systems (ICES) 2008, San Francisco, California, USA, paper 2009-01-2410 (2009)
11. "Margin Philosophy for Science Assessment Studies", ESA Document SRE-PA/2011.097/, Issue 2.1 (2016)

**Publisher's note** Springer Nature remains neutral with regard to jurisdictional claims in published maps and institutional affiliations.

## Authors and Affiliations

**G. Morgante**<sup>1</sup>  · **L. Terenzi**<sup>1</sup> · **L. Desjonqueres**<sup>2</sup> · **P. Eccleston**<sup>2</sup> · **G. Bishop**<sup>2</sup> · **A. Caldwell**<sup>2</sup> · **M. Crook**<sup>3</sup> · **R. Drummond**<sup>2</sup> · **M. Hills**<sup>3</sup> · **T. Hunt**<sup>4</sup> · **D. Rust**<sup>4</sup> · **L. Puig**<sup>5</sup> · **T. Tirolien**<sup>5</sup> · **M. Focardi**<sup>6</sup> · **P. Zuppella**<sup>7</sup> · **W. Holmes**<sup>8</sup> · **J. Amiaux**<sup>9</sup> · **M. Czupalla**<sup>10</sup> · **M. Rataj**<sup>11</sup> · **N. C. Jessen**<sup>12</sup> · **S. M. Pedersen**<sup>12</sup> · **E. Pascale**<sup>13</sup> · **E. Pace**<sup>14</sup> · **G. Malaguti**<sup>1</sup> · **G. Micela**<sup>15</sup>

<sup>1</sup> INAF - OAS Bologna, via P. Gobetti, 93/3, 40129 Bologna, Italy

<sup>2</sup> RAL Space, STFC Rutherford Appleton Laboratory, Harwell Campus, Didcot OX11 0QX, UK

<sup>3</sup> RAL Technology, STFC Rutherford Appleton Laboratory, Harwell Campus, Didcot OX11 0QX, UK

<sup>4</sup> Mullard Space Science Laboratory UCL, Holmbury St. Mary, Dorking, Surrey RH5 6NT, UK

<sup>5</sup> ESA-ESTEC, Keplerlaan 1, 2201, AZ, Noordwijk, The Netherlands

<sup>6</sup> INAF - Osservatorio Astrofisico di Arcetri, Largo E.Fermi 5, I-51025 Florence, Italy

<sup>7</sup> CNR-IFN, via Trasea 7, 35131 Padova, Italy

<sup>8</sup> Jet Propulsion Laboratory, 4800 Oak Grove Dr, Pasadena, CA 91109, USA

<sup>9</sup> CEA, Paris Saclay, 91191 Gif-sur-Yvette, France

<sup>10</sup> FH Aachen University of Applied Sciences, Bayernallee 11, 52066 Aachen, Germany

<sup>11</sup> CBK, Bartycka 18A, 00-716, Warsaw, Poland

<sup>12</sup> National Space Institute (DTU Space), Technical University of Denmark, Lyngby, Denmark

<sup>13</sup> Università di Roma La Sapienza, Piazzale A. Moro 5, Rome, Italy

<sup>14</sup> Università degli Studi di Firenze - Dipartimento di Fisica e Astronomia, 50125 Florence, Italy

<sup>15</sup> INAF - Osservatorio Astronomico di Palermo, Piazza del Parlamento 1, 90134 Palermo, Italy